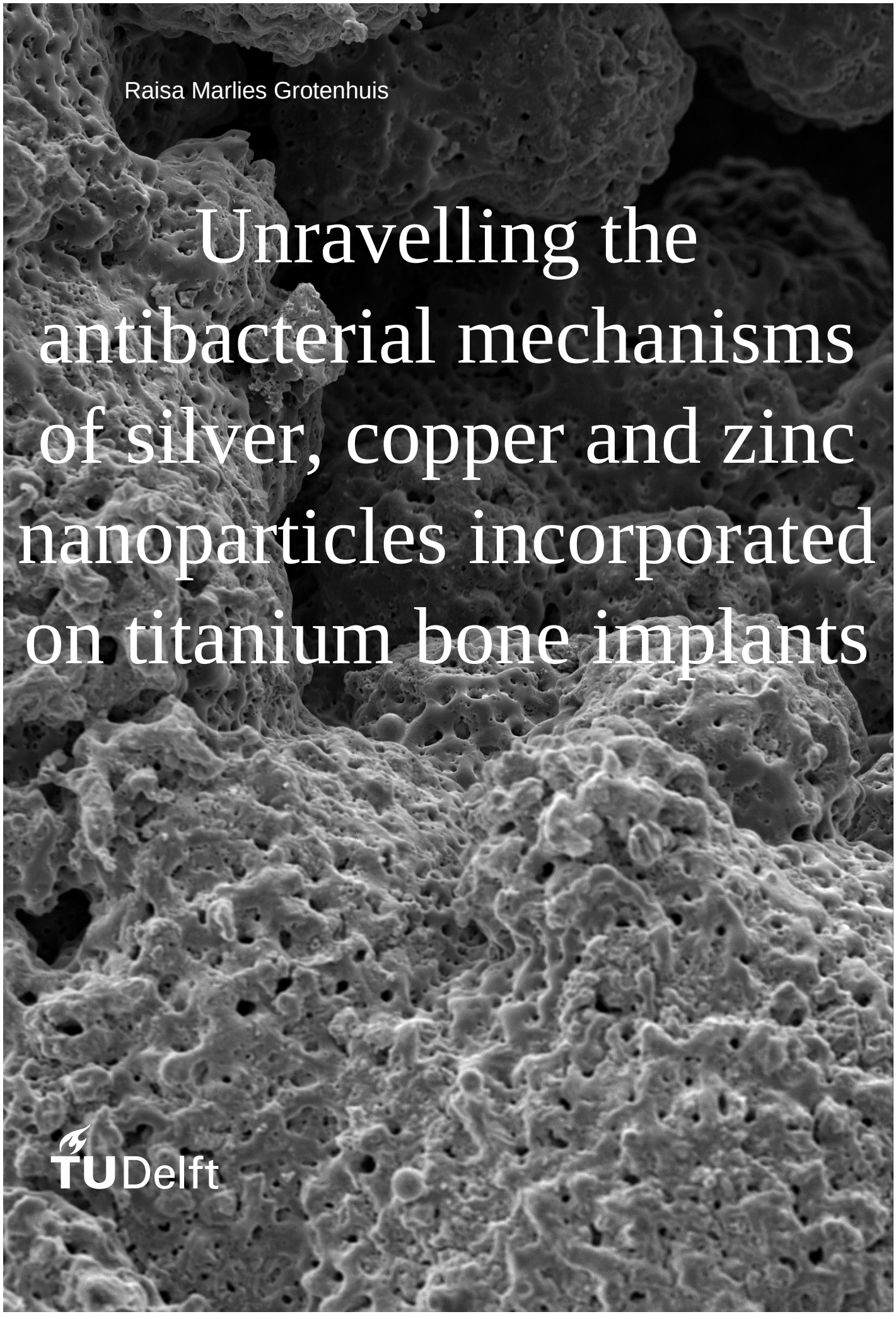

Raisa Marlies Grotenhuis

Unravelling the antibacterial mechanisms of silver, copper and zinc nanoparticles incorporated on titanium bone implants

TU Delft

Unravelling the antibacterial mechanisms of silver, copper and zinc nanoparticles incorporated on titanium bone implants

By

R. M. Grotenhuis

4604180

in partial fulfilment of the requirements for the degree of

Master of Science

in Biomedical Engineering

at the Delft University of Technology,

to be defended publicly on Tuesday September 24 at 11 AM.

Supervisor:	Ir. Ingmar van Hengel,
	Dr. ir. Iulian Apachitei
Thesis committee:	Prof. dr. ir. A. Zadpoor,
	Dr. ir. Peter-Leon Hagedoorn.

This thesis is confidential and cannot be made public until September 30, 2021.

An electronic version of this thesis is available at http://repository.tudelft.nl/.

TU Delft

Abstract

Background. The past four decades, the problem of resistant bacteria has emerged. As a result of biofilm formation of (resistant) bacteria on the implant, more implant-associated infections (IAI) occurred. This has caused an increase in orthopaedic implant revisions, causing a high burden of disease. To overcome the rising problem of resistance, many studies have focused on new antibacterial agents, such as Ag, Cu, and Zn nanoparticles (NPs) incorporated on titanium (Ti6Al4V) implants. It is known they show antibacterial effects. It is, however, unknown what causes the antibacterial effects of these metals incorporated on titanium implants. This study aims to unravel the antibacterial mechanisms of titanium implants bearing Ag, Cu or Zn NPs behind the *in vitro* antibacterial effects against methicillin-resistant *Staphylococcus aureus* (MRSA).

Methods. To obtain an implant surface bearing Ag, Cu or Zn NPs; porous Ti6Al4V implants and solid Ti6Al4Nb discs were treated by plasma electrolytic oxidation (PEO). The PEO electrolyte consisted of calcium acetate, calcium glycerophosphate, and Ag, Cu or Zn NPs. The surface morphology was visualized by scanning electron microscopy (SEM) and its chemical composition by energy dispersive X-ray spectroscopy (EDS). All implant groups contained either Ag, Cu or Zn NPs and were tested on its antibacterial leaching activity against MRSA by a zone of inhibition experiment. In addition, the antibacterial effects as a result of contact killing were examined by a direct contact assay. Porous and solid surfaces were compared to reveal the differences in their contact killing properties. Moreover, the porous implants were incubated for 2 h and 24 h. Furthermore, the generation of reactive oxygen species (ROS) of the implant with and without inoculation of bacteria was measured by electron paramagnetic resonance (EPR) for forty minutes. ROS generation after inoculation with bacteria was tested in two ways: (1) the implant was placed in a solution of bacteria PBS after which ROS generation was directly measured in 100 mM DMPO, and (2) the implant with bacteria in BHI was incubated for 2 h after which the implant was placed in 100 mM DMPO to examine ROS generation of the implant with adherent bacteria.

Results. PEO processing resulted in four biofunctionalized groups: PT, PT+Ag, PT+Cu, and PT+Zn. The presence of Ag, Cu and Zn NPs was confirmed by SEM and EDS. The antibacterial leaching activity was only observed in PT+Ag. In addition, porous implants showed better contact killing properties than solid discs. All biofunctionalized groups were significantly different from a non-treated (NT) implant considering contact killing in 24 h. Moreover, ROS generation was observed in all biofunctionalized implants. However, solely PT+Cu was significantly different from a NT implant. Furthermore, the EPR results showed that bacteria generate ROS. In all biofunctionalized groups, however, ROS decreases when bacteria are added. In all groups, the ROS generation of adherent bacteria to the implants showed higher intensity than the ROS generation of bacteria in PBS in contact with the implant.

Conclusion. Antibacterial surfaces incorporated with Ag NPs show most antibacterial leaching effects, attributed to the ion release of Ag. Furthermore, it is assumed that direct contact killing of Cu is a cause of ROS generation of an implant bearing Cu NPs.

Contents

1 Introduction

Bacterial infection at the site of orthopaedic implants has become a major problem in the medical world [1]: approximately 2% of all orthopaedic implants become infected, known as implant-associated infections (IAI) [2]. Moreover, there has been a marked increase in the prevalence of obesity in addition to a rapid increase in an aging population worldwide, both contributing to more people getting bone diseases such as hip osteoarthritis (OA) [3] and osteoporosis (OP) leading to a higher demand for implants. In the past three decades, there has been an increase in total hip replacements (THR) of 14% [1]. Unfortunately, a THR, as well as implants at other locations in the body, is associated with IAI since bacteria can adhere to the surface, colonize and form a biofilm [1], [4]. A biofilm is a community of bacteria enclosed by a slimy capsule. This capsule provides glucose and protects bacteria against phagocytes [5] which results in higher stress resistance of bacteria and higher probabilities for infections. Infections are the main cause for removal of the implant which causes a high burden of disease [4].

As a result of the increasing prevalence of infections, many studies focused on preventing infections near the implant in the past years. Preventing infections can be achieved by treating surfaces on titanium implants using several techniques such as Plasma Electrolytic Oxidation (PEO) and nanotube coating [6]. These coatings can contain a wide variety of antibacterial agents such as antibiotics and metals. Each study investigating the antibacterial performance of titanium implants considers three criteria: (1) killing bacteria on the surface, (2) minimize toxicity to human cells and (3) overcome the rising problem of bacteria resistant to antibiotics. The latter has caused that many studies focused on finding new antibacterial agents to overcome resistance looking into the antibacterial effects of silver (Ag), copper (Cu) and zinc (Zn) nanoparticles (NPs), all of which are known to be antibacterial [7].

Before studying the antibacterial mechanisms of Ag, Cu, and Zn, this study was focused on the antibacterial effects of those metals incorporated on porous titanium implants. All experiments were tested on the methicillin-resistant *Staphylococcus aureus* (MRSA) bacteria, the most prominent in hospital infections. It showed contradictory evidence that Cu and Zn incorporated on titanium implants show no antibacterial effects, whereas literature suggests otherwise. The method for incorporating NPs on the titanium surface was PEO. PEO produces an electrical current discharging the plasma of the outer surface of the titanium implant causing NPs to adhere [8]. As a result of the lacking antibacterial effect of Cu and Zn, a literature study [9] revealed that there are no studies on the antibacterial mechanisms of Ag, Cu and Zn NPs incorporated on porous titanium implants.

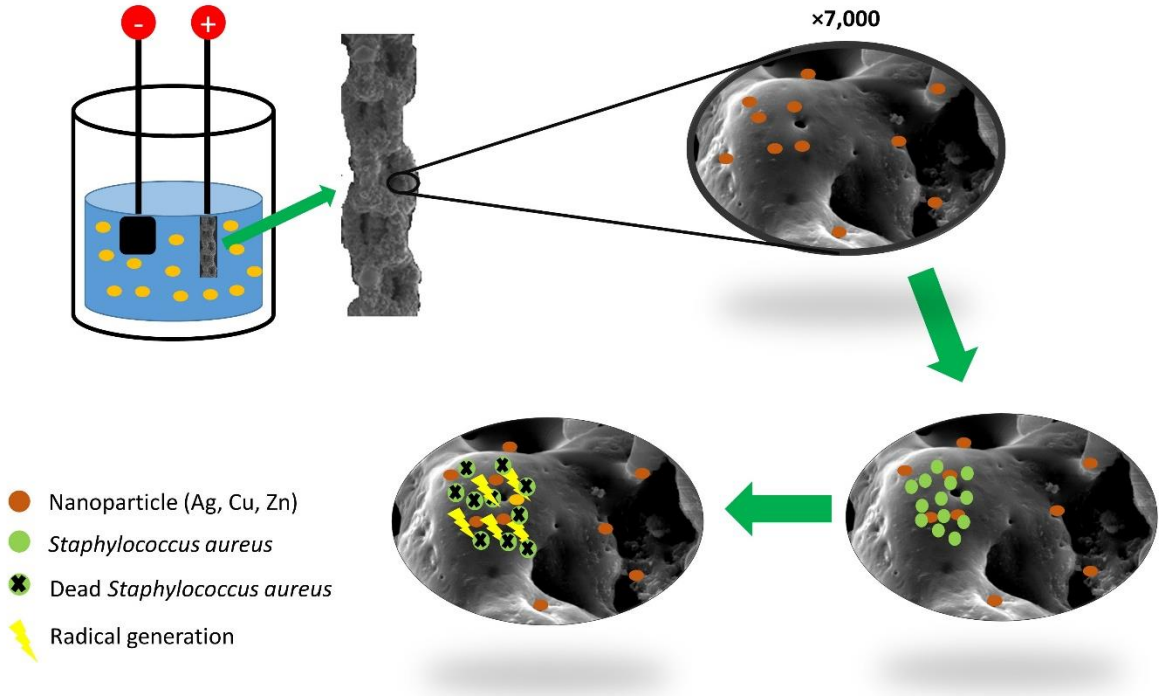

Figure 1. *Graphical abstract of this study. From top left in chronological order: (1) biofunctionalized implants are obtained by a process of PEO, (2) nanoparticles are stuck to the surface of the implant, shown by a magnification of ×7,000, (3) the implants are inoculated with Staphylococcus aureus, (4) generation of radicals (reactive oxygen species) and killing upon direct contact were studied in order to unravel the antibacterial mechanisms of Ag, Cu and Zn NPs.*

The few studies focusing on antibacterial mechanisms of Ag, Cu and Zn NPs (in solution) do suggest that two antibacterial mechanisms play a role: ion release killing [10], [11] and generation of reactive oxygen species (ROS) [12], [13]. Ion release killing is killing after the release of ions from the metal and penetration into bacteria. ROS generation is the radical formation of the implant being toxic to bacteria [9]. In addition to the antibacterial mechanisms, it was found that Cu shows best antibacterial activity as a result of contact killing [14]–[16], while Ag can release ion causing bacterial killing [10], [11]. The latter does not require actual contact between the metal and the bacteria, whereas the first does. Furthermore, Ag, Cu, and Zn can generate ROS which could be lethal to bacteria [12], [13]. In this thesis, we aimed to unravel the mechanisms of action of Ag, Cu and Zn NPs incorporated on titanium 3D printed implants: ROS generation was measured by Electron Paramagnetic Resonance (EPR) and contact killing by a direct contact assay. A graphical overview of this study is shown in **Figure 1**. Additionally, a comparison between solid and porous implants was made in direct contact killing in order to reveal the differences in antibacterial contact killing effects between porous and solid surfaces. Finally, we tried to correlate the antibacterial effects of Ag, Cu, and Zn to their antibacterial mechanisms. Knowing this can be useful for further exploring and creating coatings on titanium implants since it gives insights on how specific particles on coatings respond to bacterial adhesion. This can improve knowledge on antibacterial agents and thereby the qualities of coatings on titanium implants. This is of high importance since resistance against antibiotics is becoming a large problem.

2 Materials & Methods

An overview of the setup of the study is given in **Table 1.**

Table 1. *Overview of setup of the study.*
Abbreviations:
PEO = Plasma electrolytic oxidation, SEM = Scanning electron microscopy, EDS = Energy dispersive X-ray spectroscopy, ZOI = Zone of inhibition, ICP-MS = Inductively coupled plasma mass spectroscopy, EPR = Electron paramagnetic resonance.

Section	Goal	Method	Protocol in Appendix
Preparation of samples	Preparing discs for PEO processing	Grounding and washing	-
	Preparing wires for PEO processing	3D printing and washing	-
Synthesis of surface	Incorporation of electrolyte containing NPs onto TiO_2 layer	PEO	Protocol 1
Surface morphology	Visualization of surface and chemical composition	SEM and EDS	Protocol 2
Antibacterial activity	Antibacterial leaching activity of the implants	ZOI	Protocol 3
	Testing whether bacteria are killed upon direct contact	Direct contact assay	Protocol 4
	Measuring ROS generation of biofunctionalized implants	EPR	Protocol 5
	Measuring ROS generation in bacteria in contact with biofunctionalized implants	EPR	Protocol 6

2.1 Preparation of porous implants and solid discs

2.1.1 Preparation of solid discs

Titanium (Ti6Al4Nb) discs of diameter 21.8 mm, thickness 7.9 mm and surface area 373,3 mm^2 (**Figure 2**) were obtained from ACNIS International (France). First, the surface of the discs was ground with successive 180, 320, 800 and 1200 SiC abrasive paper (Struers, Denmark) on both circular sides for two minutes. After, the discs were washed in acetone and sonicated for five minutes. Subsequently, the discs were kept in 96% ethanol and deionized water for five minutes. This way, the discs are prepared for PEO processing.

2.1.2 Preparation of porous implants

The implants (**Figure 2**) were designed by van Hengel [17] in the Additive Manufacturing Lab (TU Delft, Delft, The Netherlands). A Selective Laser device (SLM-125, Realizer, Borchem, Germany) with Ytterbium fibre laser (YLM-400-AC, IPG, Photonics Corporation, Oxford, United States) was used. Medical grade (ELI, grade 23) Ti6Al4V spherical (10-45 nm) powders (AP&C, Boisbriand, Quebec, Canada) were used for fabrication. The Selective Laser Melting (SLM) manufactured implants had a diameter of 0.5 mm and a length of 40 mm. After manufacturing, the implants were ultrasonically cleaned in acetone, 96% ethanol and deionized water for five minutes each, prior to PEO treatment.

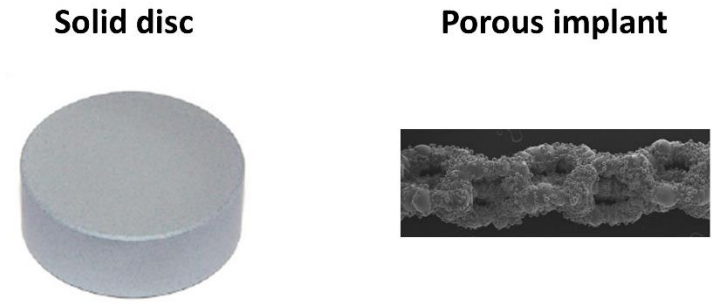

Figure 2. *Solid disc and porous implant.*

2.2 Synthesis of antibacterial implant surfaces by plasma electrolytic oxidation

2.2.1 PEO setup

The PEO setup consists of an AC power supply (50Hz, type ACS 1500, ET Power Systems Ltd., Chesterfield, United Kingdom), a data acquisition board (SCXI, National Instruments, Austin, Texas, United States), a thermostatic bath delivering cooling liquid and an electrolytic cell with two electrodes.

2.2.2 PEO procedure

The procedure was performed as described by Necula (2013) [18]. The PEO setup is at the Additive Manufacturing lab (TU Delft, Delft, The Netherlands). Calcium glycerophosphate (Ca-GP), calcium acetate (CA) and metal NPs: (1) Ag NPs (colloidal), (2) Cu NPs (40-60 nm) and (3) Zn NPs (40-60 nm) were suspended in an electrolyte of 800 mL (overview of included samples in **Table 2**). Ag and Zn NPs were purchased from Sigma-Aldrich (Saint Louis, Missouri, The United States) and Cu NPs from Skyspring Nanomaterials (Houston, Texas, The United States). Zn NPs can be spontaneously combustible and should, therefore, be weighted in a GloveBox (MBraun, Garching, Germany) to prevent contact with oxygen. The electrolyte was sonicated two times five minutes and continuously stirred at 500 rpm in order to obtain a homogenous dispersion. Furthermore, the electrolyte was cooled in order to obtain a temperature below 10 ˚C. During the process, the implants functioned as an anode (**Figure 3**). A stainless steel ring-shaped cathode was placed in the electrolyte before applying the current. The titanium implants or discs (Ti6Al7V) were fully immersed in the electrolyte. The current density was set on 20 A/dm^2, being equal to 2,543 mA for the discs and 389 mA for the implants. The duration of the process was five minutes. During the PEO process, oxidation-reduction reactions induce thickening of the TiO_2 layer (**Figure 3**) and pores were formed by plasma discharges. The voltage-time transients were recorded during the procedure. After PEO treatment, each wire was cut in pieces of length 10 mm, called implants.

Table 2. *Overview of experimental groups.*

Surface treatment	Full name	Ca GP (g/L)	CA (g/L)	Ag NPs (g/L)	Cu NPs (g/L)	Zn NPs (g/L)
NT	Non-treated	0	0	0	0	0
PT	PEO-treated	4.2	24	0	0	0
PT + Ag	PEO-treated with Ag NPs	4.2	24	3	0	0
PT + Cu	PEO-treated with Cu NPs	4.2	24	0	3	0
PT + Zn	PEO-treated with Zn NPs	4.2	24	0	0	3

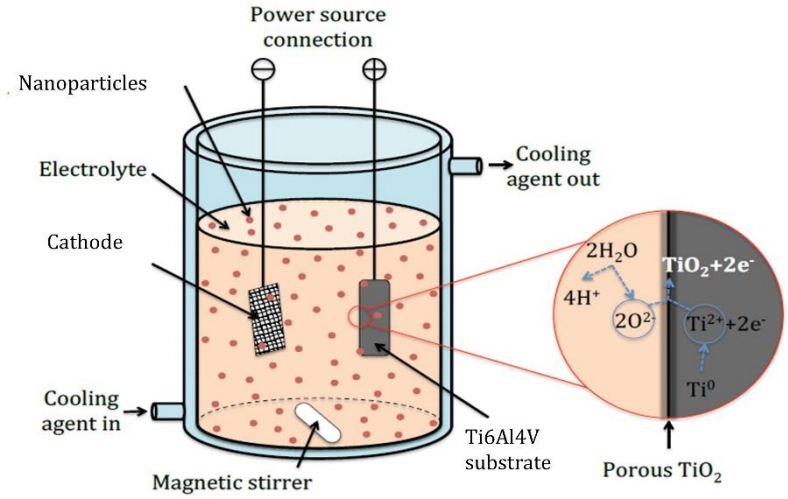

Figure 3. *Electrolytic cell. Enlargement explains oxidation-reduction reactions which forms the TiO_2 layer* [18].

2.3 Surface morphology and chemical composition of the surface

Surface morphology and chemical composition of the implants were observed by Scanning electron microscopy (SEM) and Energy dispersive X-ray spectroscopy (EDS). SEM JSM –IT100 (JEOL, Tokyo, Japan) had an electron beam energy ranging from 5 to 20 kV and a working distance of 10 mm. Before SEM imaging, the implants were coated with a gold layer for improvement of electrical conductivity. In addition, the chemical composition of the surface of the implants was analyzed by EDS on a specific point on the surface.

2.4 Antibacterial activity

In literature, three modes of action were found: ROS generation in bacteria, contact killing and ion release killing [11], [19]–[21]. Each antibacterial mode can be tested; contact killing can be examined by a direct contact assay, ion release by ICP-MS and ROS generation by EPR [22]. Prior to examining the mechanisms, the antibacterial effects were tested by a zone of inhibition (ZOI) experiment after which the adherent bacteria were visualized.

2.4.1 Preparation of bacterial inoculum

For bacterial assays, a USA300 strain of MRSA was cultured on a blood agar plate (BD, Franklin Lakes, United States) for 24 h at 37 ˚C. After, a colony of the USA300 strain was selected and dissolved in a solution of Tryptic Soy Broth (TSB) after which it was incubated at 37 ˚C while shaking at 140 rpm until the Optical Density (OD), measured by a spectrophotometer (Genesys 20 Thermospectronic, Thermo Fisher Scientific, Waltman, United States), increased to a minimum of 0.3, being in a log phase of growing.

2.4.2 Zone of inhibition

The ZOI assay was performed in order to determine the *in vitro* antibacterial leaching activity of the implants. This assay is based on the Kirby Bauer Diffusion method [23].

The inoculum was diluted in order to obtain a solution with an OD of 0.01 (~10^7 CFU(colony forming units)/mL). After it was swapped homogenously over a Lucia Broth (LB) agar plate (**Figure 4c**) and the implants, three of each group, were placed on top of it (**Figure 4d**). After, the plates were incubated at 37 ˚C for 24 h. Next, images of the plates (**Figure 4e**) were taken by Image Quant LAS 4000 (GE Healthcare, Bio-Sciences, Björkgatan, Sweden) in order to determine the zone of inhibition. For calculation of the area, the software ImageJ version 2.0.0 for Windows was used.

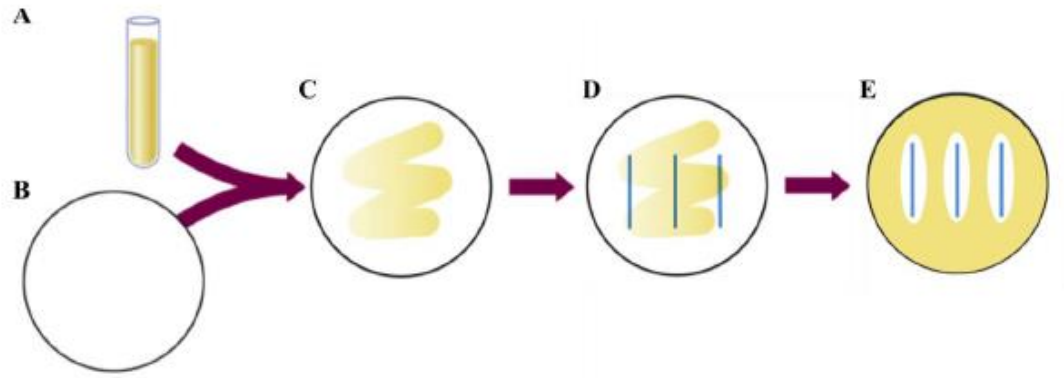

Figure 4. *Method for Zone of inhibition assay. A) bacteria dissolved in TSB. B) Empty agar plate. C) Equal distribution of bacterial solution over agar plate. D) Placing implants on agar plate with bacteria. E) Plates ready for imaging after incubation of 24 h* [24].

2.4.3 SEM imaging of adherent bacteria

For implants with adherent bacteria, the implants were inoculated with MRSA (~2.5×10^4 CFU) for 2 h after which they were fixated in a solution of 1% Glutaraldehyde, 4% paraformaldehyde and Phosphate-buffered saline (PBS). Subsequently, they were dehydrated in 50% ethanol for 15 minutes, 70% ethanol for 15 minutes and 96% ethanol for 15 minutes. After, the implants with adherent bacteria were visualized by SEM.

2.4.4 Direct contact assay

The direct contact assay was performed in order to determine the direct contact killing properties of the implants. The assay was adapted from the Japanese Industrial Standard (JIS) [25].

2.4.4.1 Preparation of porous surface

A clamp was constructed to keep four implants close together. This way, a porous surface, similar to the surface of the discs, was obtained (**Figure 5b**). This clamp was constructed at the workroom at the 3mE department of the TU Delft (Delft, The Netherlands) and consists of screws and two holders (**Figure 5a**). The two holders, made of stainless steel, were kept together by two screws (**Figure 5b-c**). The lower holder should contain holes in which screws can be screwed, which was obtained by a Flott 10 plus drilling machine (Hahn + Kolb Group, Stuttgart, Germany). The outer surface area of four implants was equal to 62.83 mm^2 (length × circumference). The ratio of the area of solid wires versus porous wires was 3.75, resulting in a working surface area of 235.6 mm^2 (62.83 × 3.75 = 235.6 mm^2) for porous implants.

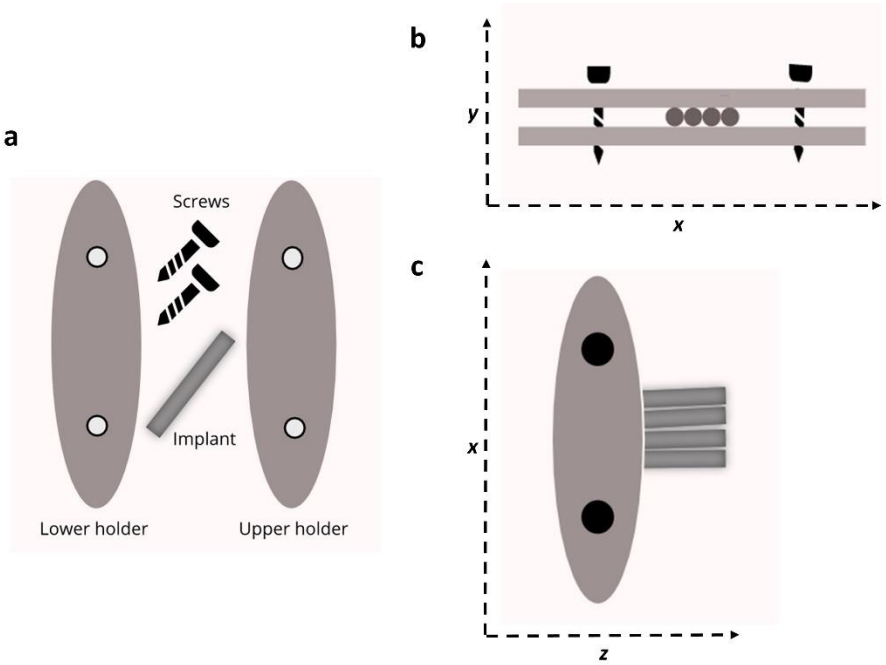

Figure 5. *Clamp for implants. a) components of the clamp, b) front view of the clamp, c) top view of clamp.*

2.4.4.2 Inoculating the discs/implants

Following the JIS that applies 1×10^2 CFU/mm^2 [25], 40 µL inoculum was pipetted over the surface of the disc (373.3 mm^2, **Figure 6**). After, a circular parafilm was placed over the disc spreading the inoculum without spillage. The discs were placed in a petri dish in a humid environment. For each condition, three discs were used. All groups were incubated at 37 ˚C.

The ratio of the surface area of solid discs versus porous implants is 1.58 (=373.3/235.6 mm^2). For that reason, the inoculum of the implants was equal to $4\times10^4/1.58 = 2.5\times10^4$ CFU (being equal to 1×10^2 CFU/mm^2, similar to the discs). The implants were placed in a clamp (**Figure 5**) prior to inoculation. The inoculum (15 µL) was pipetted over the surface of the implants. After a parafilm was placed over the surface and the implants were kept in a humid environment, similar to the discs. All groups were incubated at 37 ˚C.

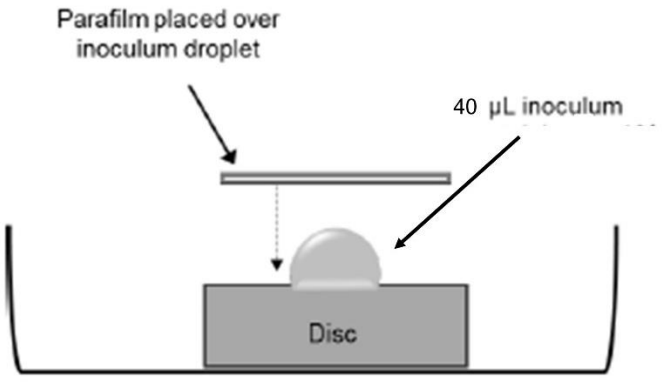

Figure 6. *Schematic diagram of direct contact assay for discs. A disc was placed in a petri dish over which a droplet of the inoculum was pipetted, covered by a parafilm. Adapted from* [18].

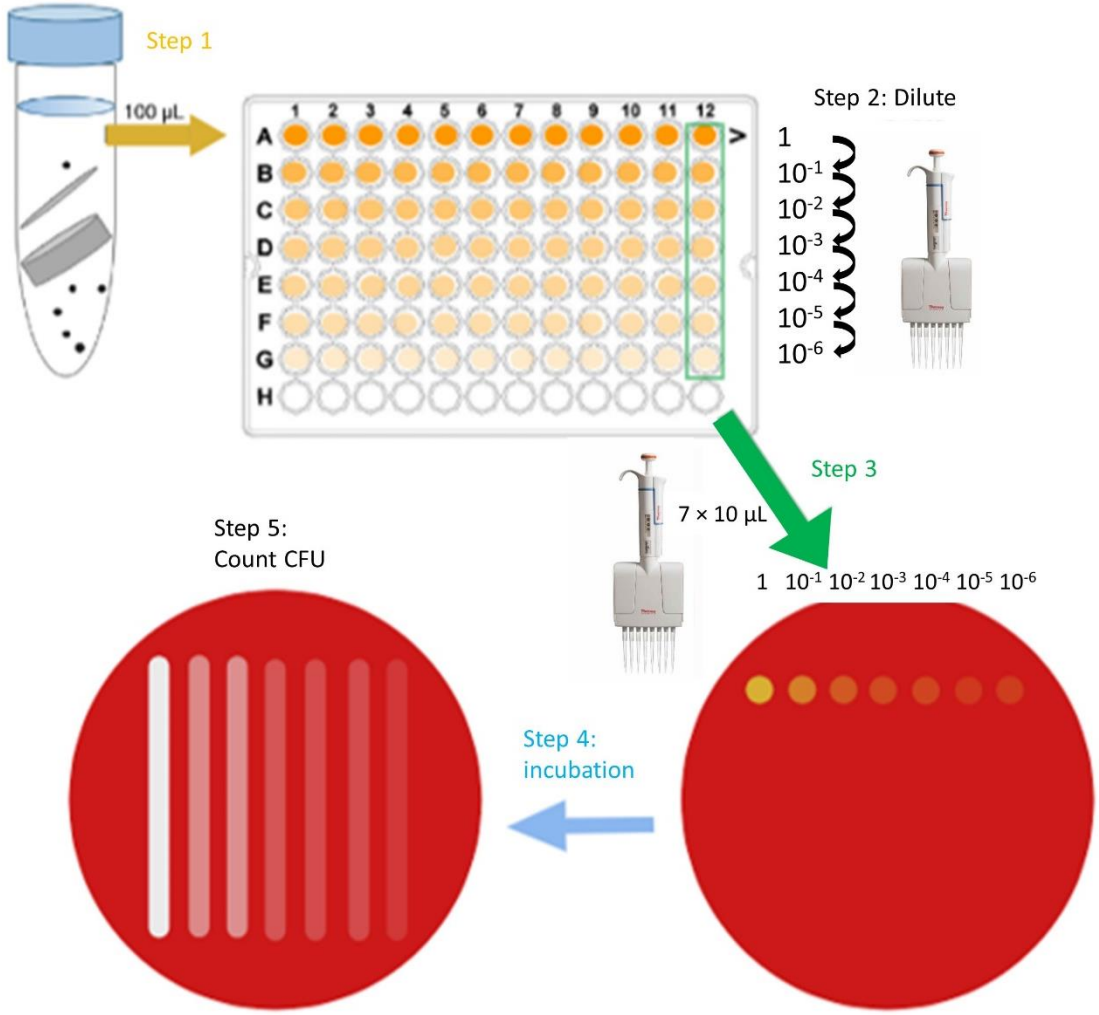

Figure 7. *Method of counting the CFU step by step.*
Step 1: pipet 100 µL of suspension in row A of 96-wells plate; step 2: Fill row B-G with 90 µL PBS and dilute each well in row A by pipetting 10 µL into row B (up to row G); step 3: Pipet row A-G of each column onto blood agar plates; step 4: Incubate; step 5: Count the CFU of one column and determine the amount of CFU.

2.4.4.3 Counting colony forming units

After incubation, each disc was placed in 5 mL PBS. Each porous implant was placed in 200 µL PBS 1.5 mL Eppendorf tube. All samples were sonicated for three minutes and vortexed for 15 seconds to remove adherent bacteria. After, sevenfold serial dilutions (10^0-10^{-6}) were made in a 96 wells plate (**Figure 7, step 2**). Subsequently, a multichannel pipet was used to pipet 10 µL of the serial dilutions onto blood agar plates (**Figure 7, step 3**) after which the plates were incubated overnight at 37 ˚C (**Figure 7, step 4**). The next day the amount of CFU was counted in order to conclude whether the disc or porous implant inhibited bacterial growth (**Figure 7, step 5**).

2.4.5 Electron Paramagnetic Resonance

The last mechanism of action is the generation of ROS. ROS generation was measured by Bruker EMX Plus, an EPR spectrometer (Billerica, Massachusetts, United States).

2.4.5.1 EPR theory

During EPR measurements (setup in **Figure 8b**), photon energy and magnetic radiation are applied. Magnetic radiation (on the *x*-axis of **Figure 8a**) can react with unpaired electrons, causing the electrons to spin up or down generating a difference in energy (ΔE). When the photon energy (*hv*) is equal to ΔE, an EPR spectrum can be obtained. The relationship between the parameters producing an EPR signal is described by **Equation 1** [26], where h is Planck's constant (6.626×10^{-34} m^2kg/s), *v* is the electromagnetic frequency, β is Bohr's magneton (89.274×10^{-24} J/T), g characterizes the angular momentum of a radical and is dimensionless, and B is the magnetic field [22], [26]. Peaks in an EPR spectrum reveal which radicals are generated on your sample.

$$\Delta E = hv = \beta g B \qquad (1)$$

2.4.5.2 EPR spectrometry

Two implants of length 0.5 cm were prepared, one for recording the baseline spectrum and one for recording radical formation. Detecting radicals requires the spin trapping agent 5,5-dimethyl-pyrroline N-oxide (DMPO) [27] (Sigma-Aldrich, St. Louis, United States) to prolong the lifetime of the radicals, making them detectable by the spectrometer. The implant was put inside a quartz capillary tube filled with 10 µL of 100 mM DMPO dissolved in PBS. ROS generation was examined in three situations (**Figure 8c**):

1. Implant without bacteria
2. Bacteria without implant
3. Implant with bacteria

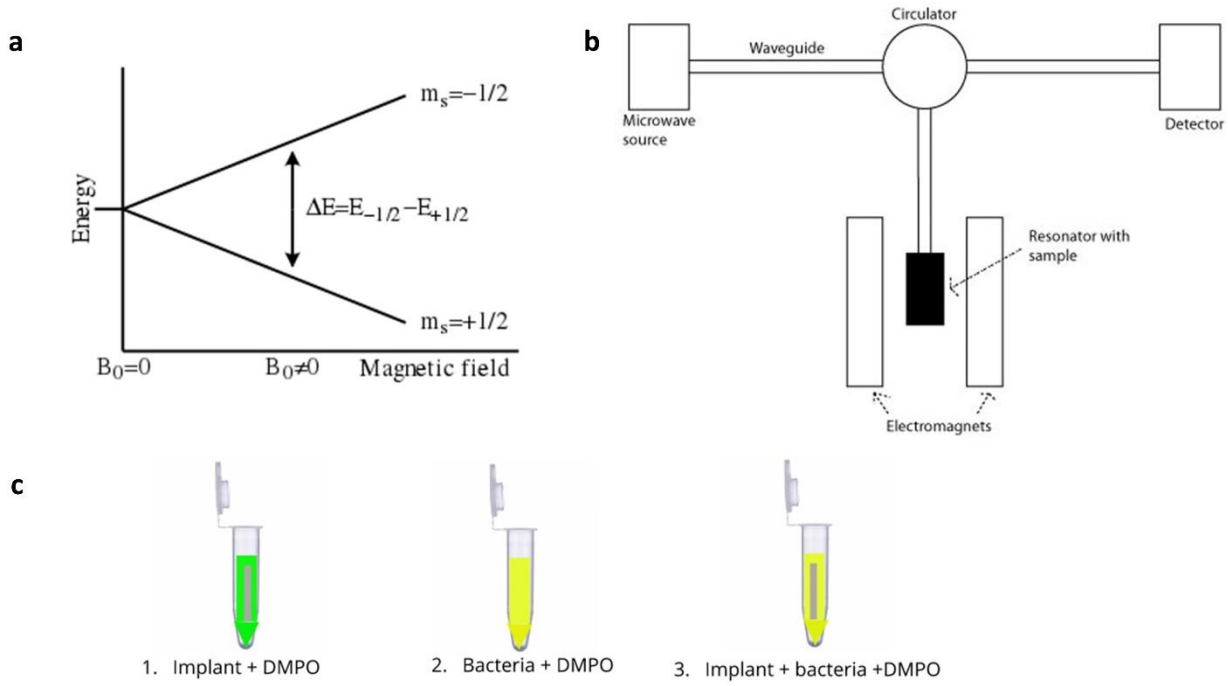

Figure 8. *Method of Electron paramagnetic resonance (EPR). a) EPR theory* [28]*, b) EPR setup, c) Groups: implant + DMPO; bacteria + DMPO; implant + bacteria + DMPO.*

ROS generation on implants in contact with bacteria (option 3) was performed using two different methods (**Figure 9**). The first method 'bacteria in PBS' measures ROS generation of the bacteria in a solution of PBS with the implant, whereas the second method 'adherent bacteria' measures adherent bacteria. For both methods, a colony RN0450 of *S. aureus* was tipped from an agar plate and dissolved in brain heart infusion (BHI) broth. The solution was incubated for 18 h at 37 ˚C while constantly shaking.

Bacteria in PBS

After incubation, the OD at 600 nm was measured. The solution was diluted up to the OD was equal to 1.0 (~ 6×10^8 CFU/mL). Next, the inoculum was centrifuged for one minute at 12,000 rpm (Eppendorf Centrifuge 5424, Hamburg, Germany) after which the BHI was replaced by PBS and vortexed. Next, 3 µL of the bacterial solution (~2×10^6 CFU), 10 µL of 100 mM DMPO and an implant of 0.5 cm was added to the capillary prior to EPR measurements (**Figure 9a**). This way the ROS generation of bacteria in solution and the implant could be measured.

Adherent bacteria

After incubation for 18 h, the OD was diluted up to 0.1 (~ 6×10^7 CFU/mL). Next, 100 µL BHI (~6×10^6 CFU) was pipetted in an Eppendorf tube. Four implants (length 0.5 cm) per group were placed in the tube and incubated for 2 h (**Figure 9b**). Subsequently, three implants were placed in 100 µL PBS and sonicated for one minute. After, serial ten-fold dilutions (10^0-10^{-6}) were pipetted on an agar plate and incubated for 24 h, followed by CFU counting in order to know the number of bacteria adhered to the implant surface (not shown in **Figure 9b**). The fourth implant from the Eppendorf tube was used for EPR measurements and was placed in a capillary in 10 µL DMPO (**Figure 9b**). This way the ROS generation of the adherent bacteria could be measured after 2 h.

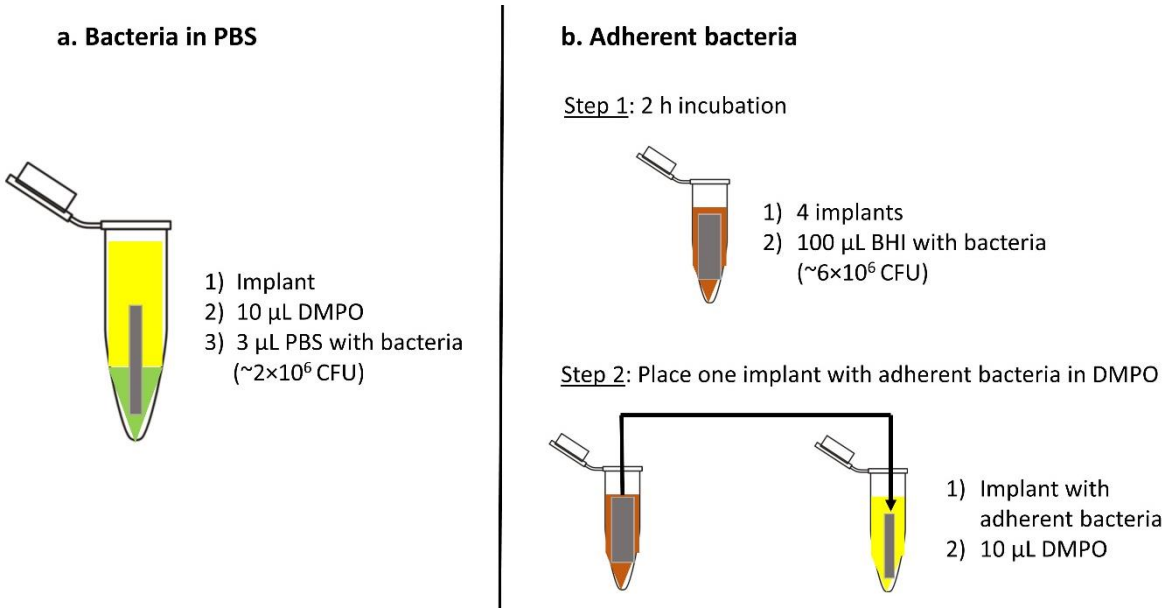

Figure 9. *Two different methods of EPR with inoculation of bacteria a) bacteria in PBS, b) adherent bacteria.*

After preparing the sample, it was placed in a cavity in between electromagnets (black rectangle in **Figure 8b**). The settings of the EPR spectrometer were as follows: 9.78 GHz frequency, 4799.3 G sweep width to detect the background spectrum, 100 G sweep width to detect the radical formation, 163.8 ms time constant, 160 ms conversion time, 1 G modulation amplitude, 100 kHz modulation frequency, 50 dB receiver gain, 10 dB attenuation, and 20 mW power. The radical generations were recorded for forty minutes, acquiring ten spectra each taking four minutes.

2.4.5.3 Data analysis

Three types of ROS were screened on the implants: the hydroxyl (·OH) radical, the methyl (CH_3) radical and the superoxide ($O_2^{\cdot-}$) radical. The characteristic spectra of the radicals were plotted by Easyspin using the parameters listed in **Table 3**. The g-value, a value describing the angular momentum of a radical, is similar for all radicals. However, the hyperfine splitting constants differ. A hyperfine splitting

constant declares the interaction of the unpaired electrons with nuclei and thereby the spacing between the peaks in the spectra, being different for each type of radical [28], as shown by **Table 3**.

The EPR spectra from Xenon (Bruker) were saved as a DSC file. A DSC file could not be read in other software; therefore, it was transferred to a CSV file by Easyspin (Version 5.2.25, a Matlab toolbox). CSV files could be read by Excel 2013 (Microsoft, Redmond, Washington, United States). After transferring files to CSV, the acquired data from the implants were compared to the EPR spectra of the radicals by overlaying plots using Matlab R2016b (Mathworks, Natick, Massachusetts, United States) and Excel 2013 (**Figure 10** overlays a spectrum from a PT+Cu implant with the ·OH radical). This way, it could be concluded what implants generated the characteristic radicals. **Figure 10** shows that this implant generates the ·OH radical, since the peaks overlap. ROS generation was examined over time by acquiring scans every ten to four minutes for 40 minutes. The ROS generation can be observed by taking the average of all scans, or by tracking one radical over time. Using the first method can miss a specific generation of a radical during the shorter period, while the latter can only track one specific radical and does not show noise. The latter is done by tracking the top of the ·OH and CH_3 peak over time. This reveals the generation of a specific radical for 40 minutes. All EPR measurements were done twice or more; therefore, all results are the average of two measurements.

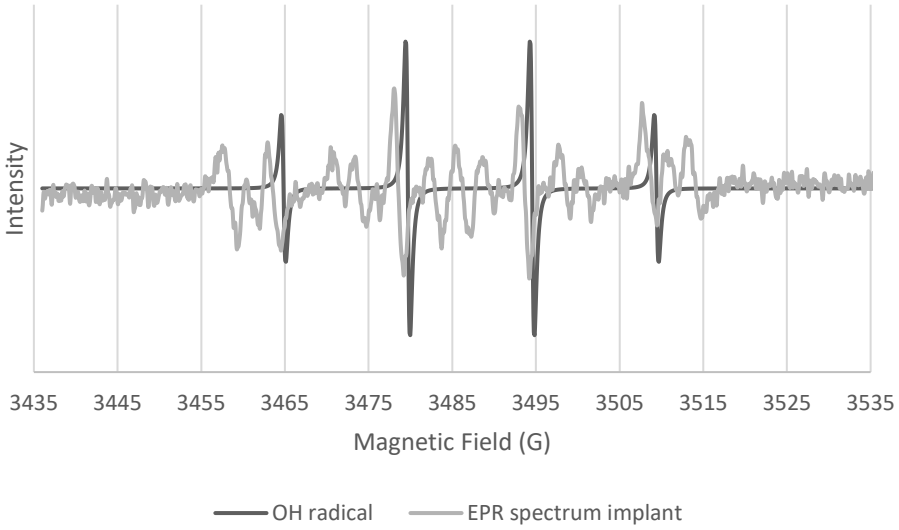

Figure 10. *Overlaying EPR spectra of ·OH radical and implant in Excel 2013.*

Table 3. *DMPO spin adduct parameters* [29].

Radical		g-value	Hyperfine splitting constants (Gauss)		
Full name	Formula		A^H	A^N	$A^{H(2)}$
Hydroxyl	·OH	2.006	14.9	14.9	-
Methyl	CH_3	2.006	23.3	16.4	-
Superoxide	$O_2^{\cdot-}$ or OOH	2.006	11.7	14.3	1.3

2.5 Statistical analysis

The statistical analysis was performed in IBM SPSS Statistics version 24 for Windows (SPSS Software, Armonk, NY, United States). One-Way ANOVA was performed for the direct contact assay as well as for the ZOI, followed by a post hoc comparisons. The 2D EPR results were analysed by a repeated measures ANOVA (Mauchly's test of Sphericity) to involve all scans. This way, it could be concluded whether there are significant differences between scans considering the groups (scans*group) and thus whether a time dependence appeared. If so, all scans should be analysed separately by a one-way ANOVA. Moreover, a one-way ANOVA was performed on the average of all scans to compare ROS generation between groups. Differences between groups are considered significant when $p<0.05$.

3 Results

3.1 Synthesis of the antibacterial surface

Figure 11 and 12 show the voltage-time transients of the solid discs and the porous implants, respectively. The voltage-time curve reveals the growth of the TiO_2 layer. In both plots, the initial voltage increase breaks at approximately 9 ± 1 s, which is called the dielectric breakpoint. The dielectric breakpoint is the moment at which the plasma of the implants discharges and the particles will be incorporated at the surface [8]. After the dielectric breakpoint, the voltage of each group linearly increased at a slower rate of 0.35 V/s. For both discs and implants, PT+Zn has the highest dielectric breakpoint, being 140 ± 5 V. The other groups have approximately similar breakpoints, being equal to 115 ± 5 V.

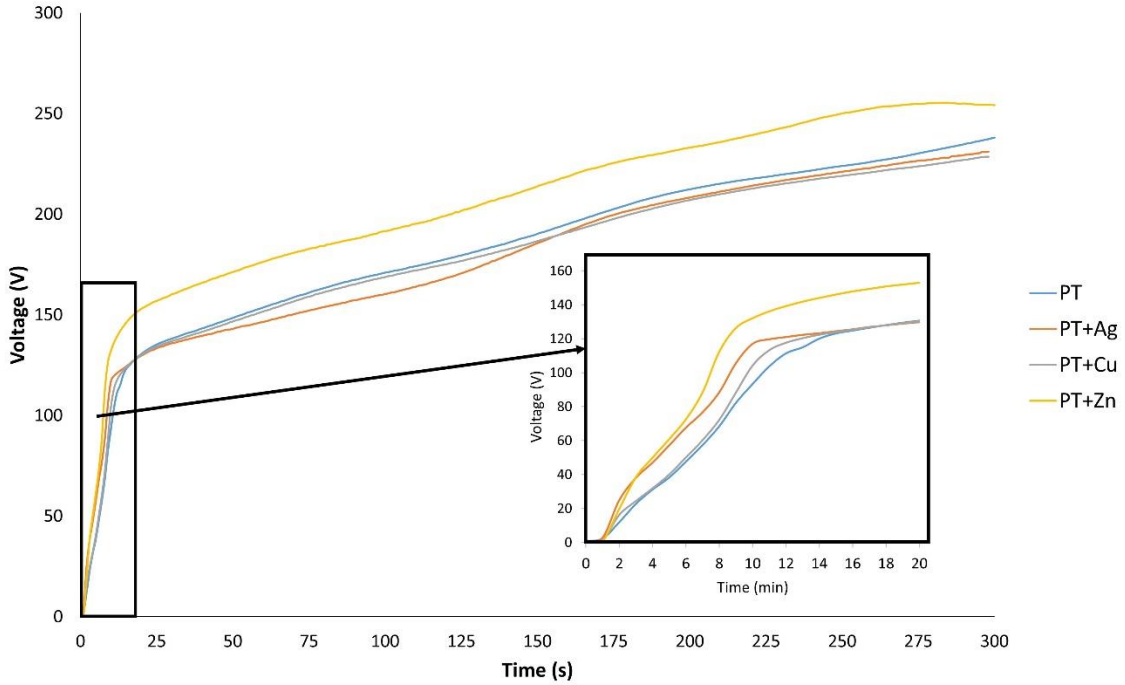

Figure 11. *Voltage-time plot of discs. Average of all PEO measurements (25 per group) was taken.*

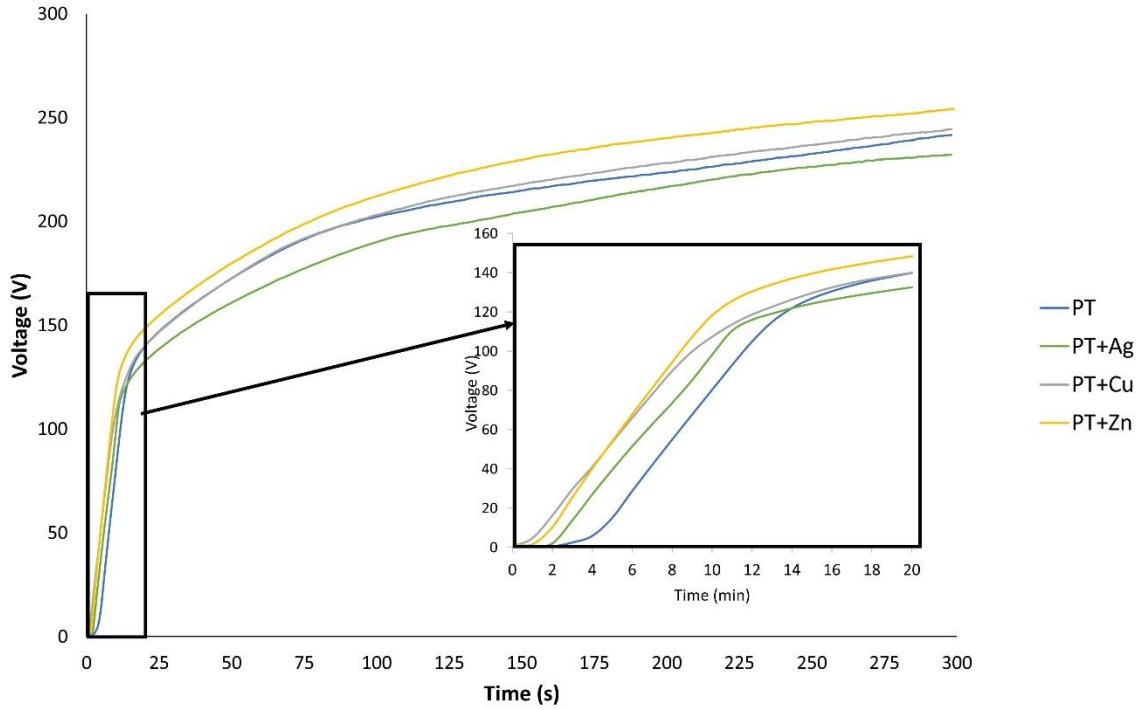

Figure 12. *Voltage-time plot of porous implants. Average of all PEO measurements (25 per group) was taken.*

3.2 Surface morphology and chemical composition

To reveal the difference in morphology of the surface between a solid disc and a porous implant, two samples were visualized by SEM: a PT+Cu disc and a PT+Zn implant in magnifications 500× and 2,000× (**Figure 13**). The porous surface shows more pores and bulges (**Figure 13b**) than the solid surface (**Figure 13d**). Furthermore, the porous surface has holes through which bacteria can flow, whereas the disc does not.

The chemical composition of the biofunctionalized implant surface can be revealed by EDS. For each implant with NPs, EDS was performed at a point on the surface on which NPs are present (**Figure 14**). In all surfaces, the elements C, O, Al, P, Ca and Ti are also present. However, the difference between surfaces is the presence of the metal NP. Ag and Cu NPs were easily found and their mass distribution was 14.38% and 27.21%, respectively (**Table 5** in Appendix 9.1). Oppositely, Zn NPs were hard to detect; its mass percentage is equal to 3.92%, showing small peaks in **Figure 14c**.

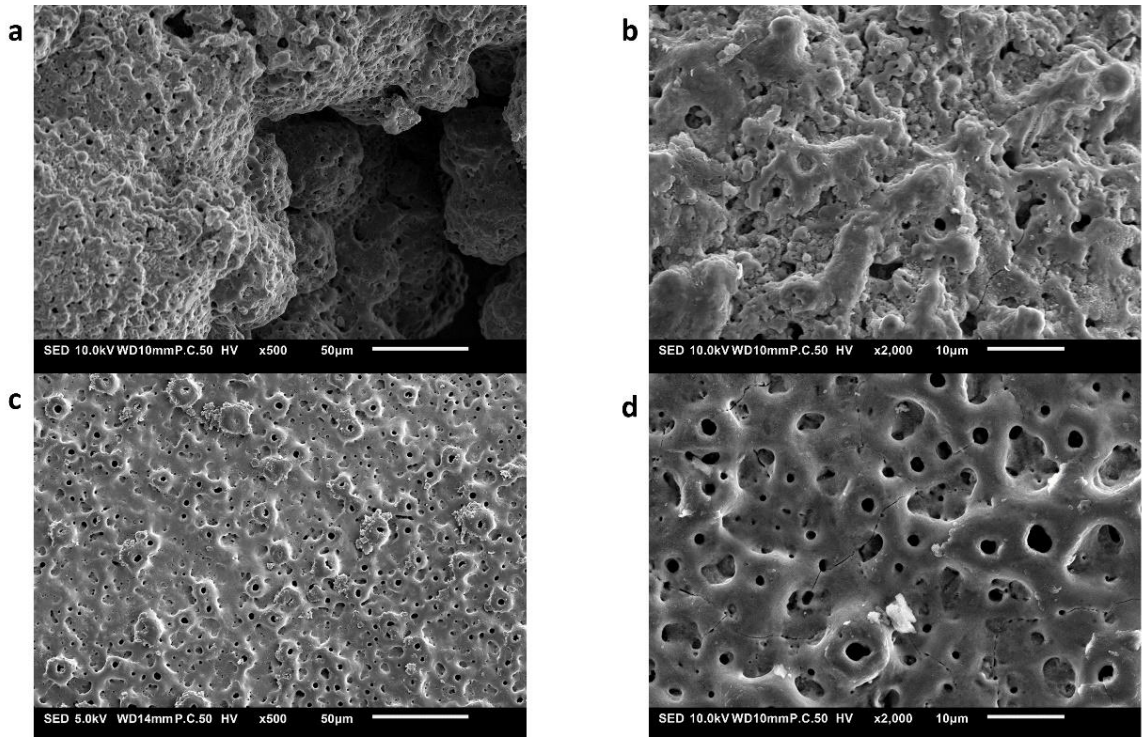

Figure 13. *SEM images a) PT+Zn implant magnification ×500, b) PT+Zn implant magnification ×2,000, c) PT+Cu disc magnification ×500, d) PT+Cu disc magnification ×2,000.*

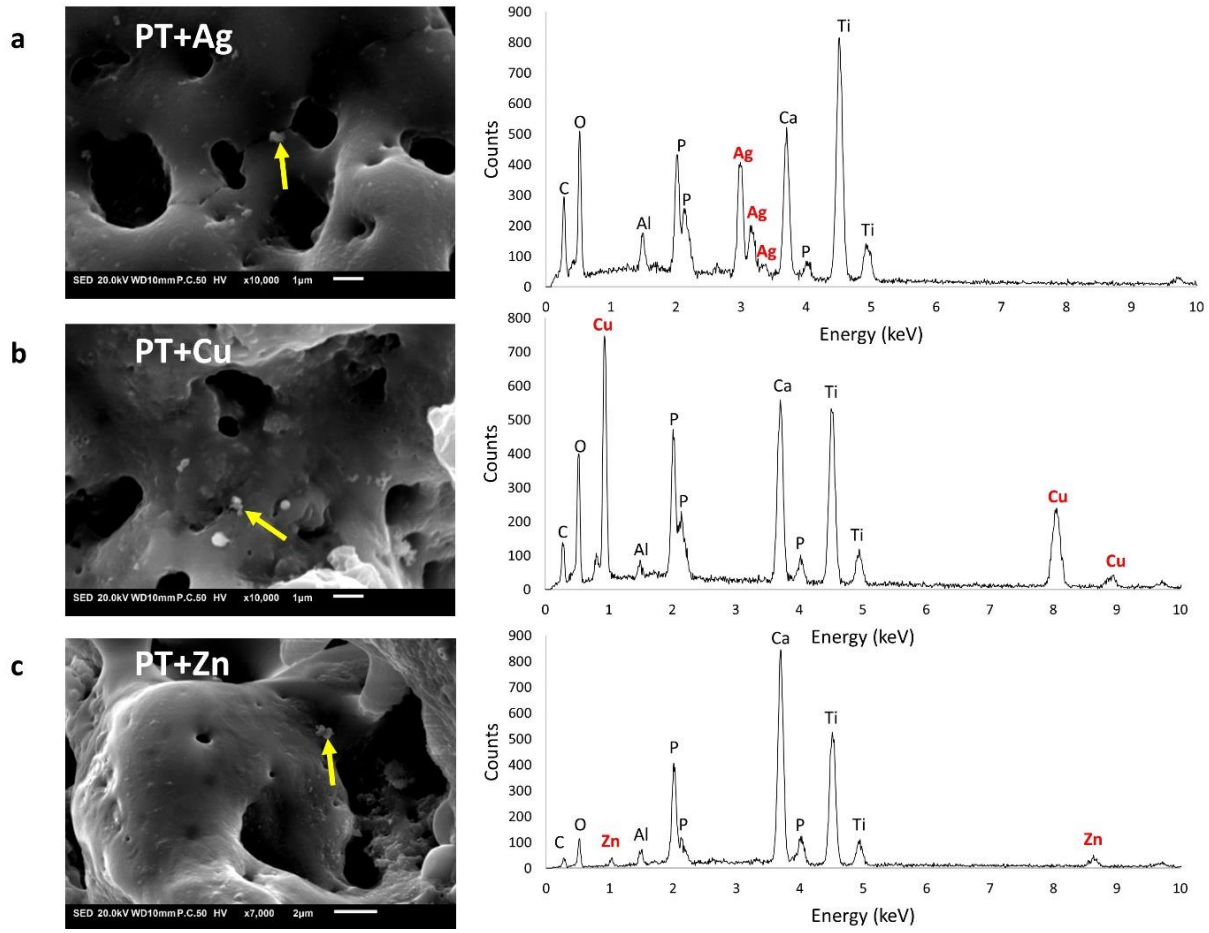

Figure 14. *SEM images with EDS spectrum of location indicated with the yellow arrow. a) PT+Ag, b) PT+Cu, c) PT+Zn.*

3.3 Antibacterial activity

3.3.1 Antibacterial leaching activity

The leaching activity of the implants was tested against MRSA USA300. The results are shown in **Figure 15**. The results imply that solely Ag NPs show antibacterial leaching activity, having a ZOI of 0.65 ± 0.2 cm^2 being significantly different from all other groups ($p<0.001$).

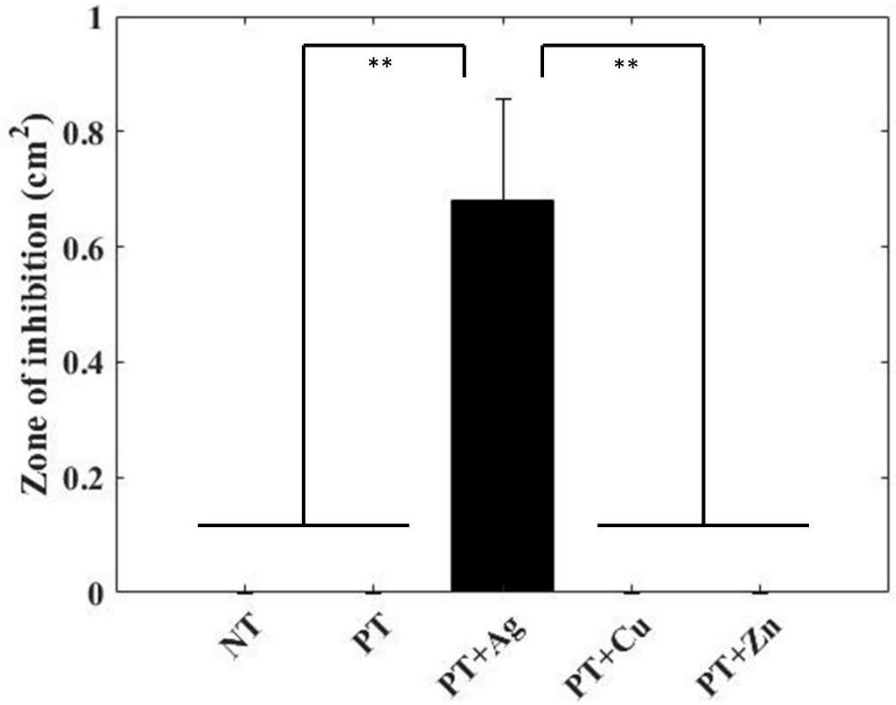

Figure 15. *Antibacterial leaching activity results (n=3, *; p<0.05, **; p<0.01).*

3.3.2 Biofilm formation

After incubation of 2 h with MRSA, implants with adherent bacteria were visualized (**Figure 16**). All groups were visualized in magnifications 2,000× and 5,000×. All implants show bacterial adhesion. However, the NT implant and PT implant (**Figure 16a and 16b**) show substantially more adherent bacteria than the PT+Ag implant and PT+Cu implant (**Figure 16c and 16d**).

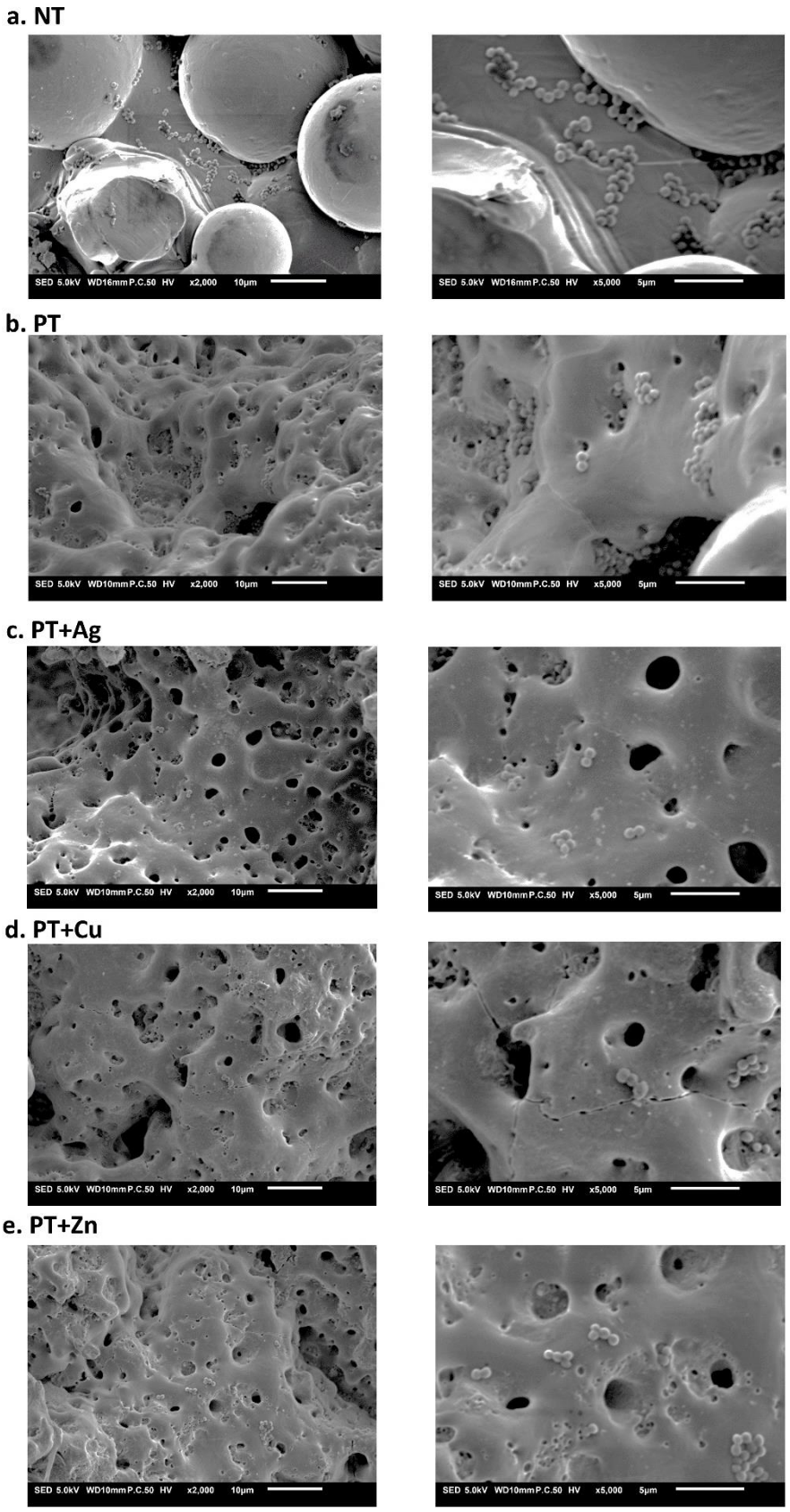

Figure 16. *SEM images with adherent bacteria after 2 h incubation. Left: magnification ×2,000, right: magnification ×5,000. a) NT implant b) PT implant, c) PT+Ag implant d) PT+Cu implant, e) PT+Zn implant*

3.3.3 Contact killing

The direct contact assay was performed on solid discs and porous implants. **Figure 17** shows the results of direct contact killing on solid discs having a contact area of 373.3 mm^2. **Figure 17a** are the results from an inoculum of 4×10^4 CFU, being equal to the JIS standard [25] and **Figure 17b** shows the results of an inoculum equal to 1×10^3 CFU. Both results do not show significant differences between groups ($p>0.129$ for all groups).

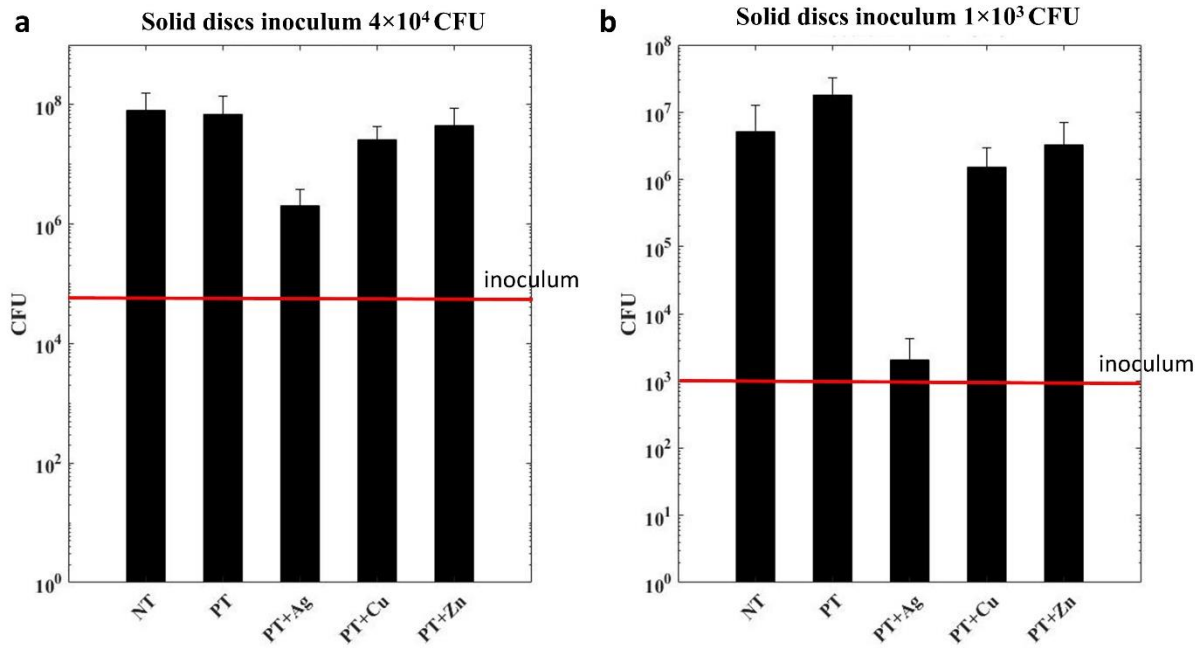

Figure 17. *Results of direct contact assay (n=3). Comparison between a) solid discs with a high inoculum (4×10^4 CFU), and b) solid discs with a low inoculum (1×10^3 CFU). No significant differences between groups.*

3.3.3.1 Solid vs. porous

Literature suggests that porous implants are more effective in killing bacteria since the surface area of a porous implant is higher than it is of a solid implant. As mentioned, the inoculum of the implants is adjusted to its porous surface area. The results of the porous implants after incubation of 24 h is shown in **Figure 18b**. For either the solid discs (**Figure 17**) and the porous implants (**Figure 18b**) PT+Ag shows most antibacterial activity. For the porous implants, the differences between all biofunctionalized implants and NT implants is significant ($p<0.001$ for all groups). However, there are no significant differences between types of biofunctionalized implants ($p>0.999$ for all groups).

3.3.3.2 Varying incubation time

In addition to solid versus porous, a distinction of incubation time of porous implants is made. Following the U.S. Environmental Protection Agency (EPA), a surface should be killing bacteria within 99.9% of the bacteria within 2 h; therefore, an incubation time of 2 h (**Figure 18a**) is compared to a longer incubation time of 24 h (**Figure 18b**). **Figure 18a** shows that after an incubation time of 2 h PT+Ag and PT+Cu show bacterial inhibition, illustrated by a decrease in the number of CFU compared to the inoculum. NT, PT and PT+Zn do not show bacterial inhibition. However, no significant differences appeared ($p>0.189$ for all groups).

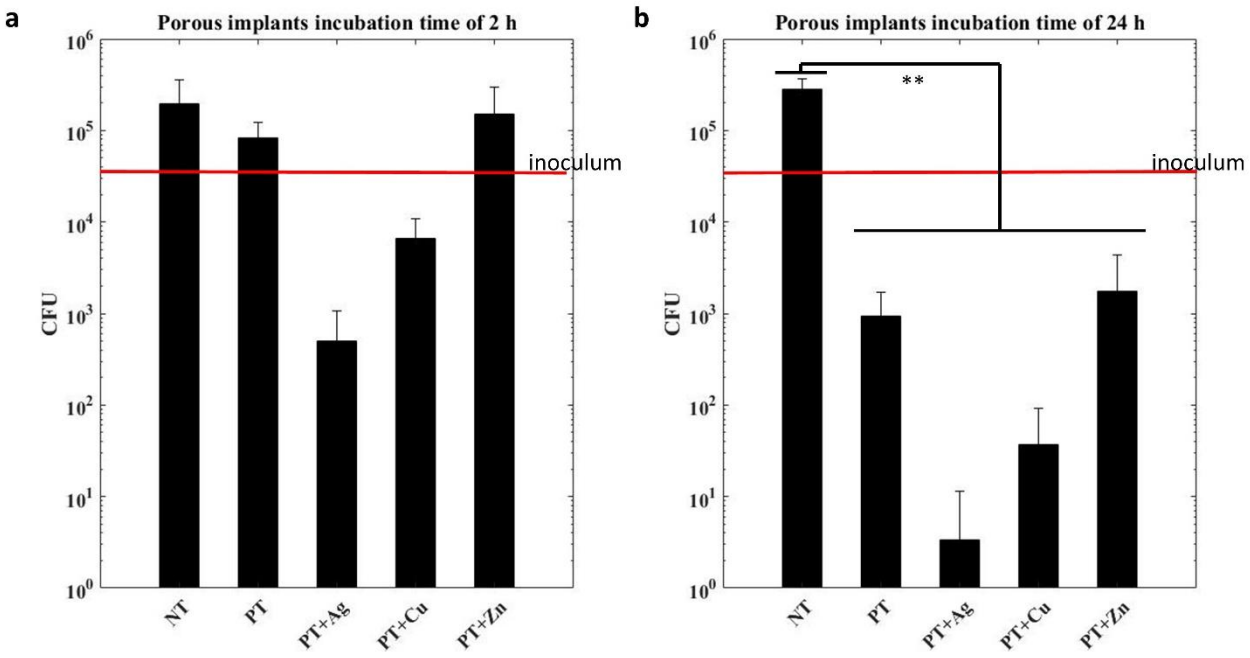

Figure 18. *Results direct contact assay (n=3, *; p<0.05, **; p<0.01) of porous implants. The red line is the amount of CFU of the inoculum (2.5×10⁴ CFU). a) incubation time of 2 h, b) incubation time of 24 h.*

3.3.4 ROS generation

3.3.4.1 ROS generation of implants

Three types of ROS were screened on the implants: the hydroxyl (·OH) radical, the methyl (CH_3) radical, and the superoxide ($O_2^{\cdot-}$) radical. The characteristic spectra of these radicals are shown in **Figure 16** as well as the spectra of the implants. The parameters used to produce the characteristic spectra of the radicals in Matlab R2016b are shown in **Table 3**. **Figure 19** shows the average of ten scans each taking four minutes. All implants except the NT implant generate the ·OH radical, indicated by the triangles. In addition, it was observed that all implants produced the CH_3 radical and that PT+Cu and PT+Zn produced the $O_2^{\cdot-}$ radical. However, the characteristic spectrum of the $O_2^{\cdot-}$ radical overlaps with the ·OH radical (**Figure 19**). As a result, it is difficult to conclude whether peaks in EPR spectra of the implants can be assigned to the ·OH radical or the $O_2^{\cdot-}$ radical. The average of all scans indicate significant differences between NT and PT+Cu (**Figure 19**). Moreover, there are no significant differences between scans (p=0.239) meaning that there is no time dependence of ·OH radical generation. **Figure 20** shows the generation of the ·OH and CH_3 radical over time. It shows that the PT+Ag and PT+Cu show an increase in ·OH during the first 8 minutes after which it becomes stable. PT shows a decrease in ·OH generation after 8 minutes. NT and PT+Zn implants show a stable production of the ·OH radical, being equal to 0.015 and 0.042 arbitrary units (a.u.), respectively. PT+Cu shows significantly more ·OH generation than NT; having values of approximately 0.07 and 0.075 a.u. (**Figure 20a**). Furthermore, all groups except PT+Cu show a stable CH_3 radical generation (**Figure 20b**): the intensity of the NT implant is between 0.01 and 0.015 a.u., whereas PT, PT+Ag and PT+Zn show values between 0.015 and 0.03 a.u. Oppositely, PT+Cu shows a decrease of CH_3 radical up to 16 minutes (from 0.048 to 0.01 a.u.) after which it becomes stable and negligibly small. The repeated measures ANOVA indicated there was a time dependence in CH_3 radical generation: during the first 8 minutes PT+Cu is significantly different from other groups. After 8 minutes, there are no significant differences between groups (**Figure 20b**).

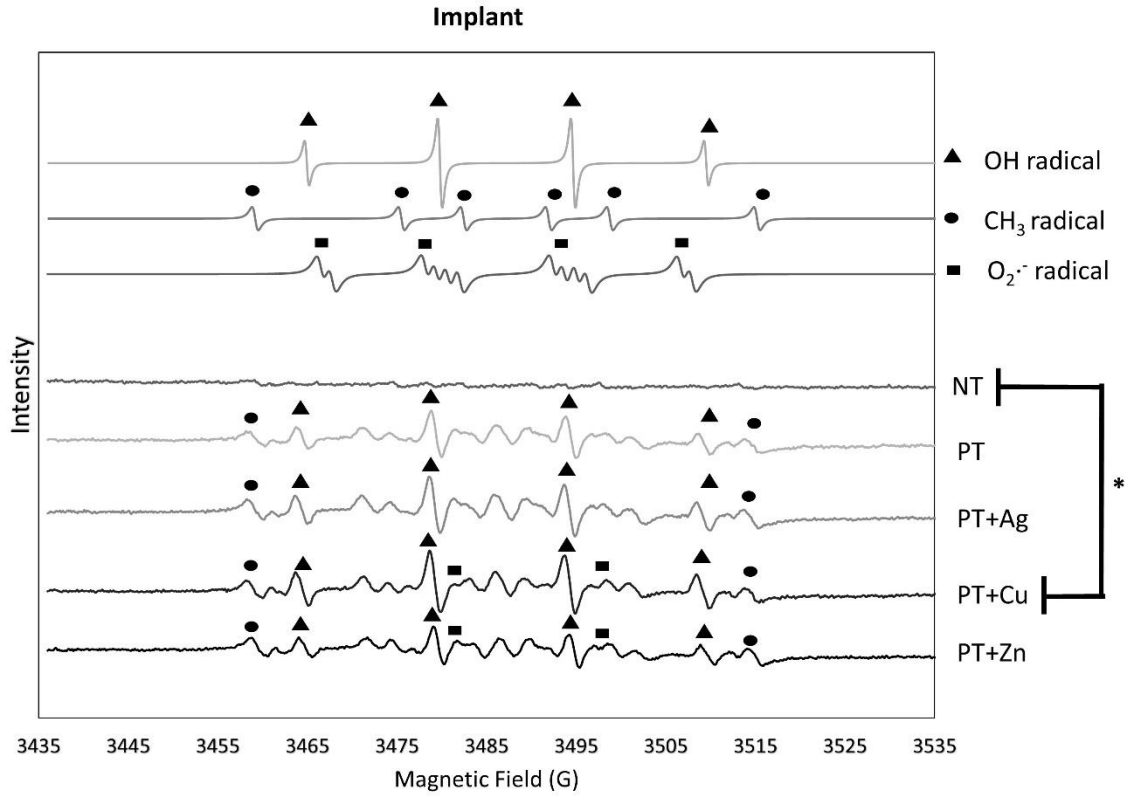

Figure 19. *ROS generation of implants (n=3, *; p<0.05, **; p<0.01).*
Top three lines represent characteristic spectra of the ·OH radical, the CH_3 radical and the $O_2^{\cdot -}$ radical (indicated by triangles, circles and rectangles, respectively). Bottom five lines represent the average of 10 EPR spectra in 100 mM DMPO of the implants. Characterisation of the radicals on implants is indicated by placing shapes (belonging to a certain radical) above each spectrum.

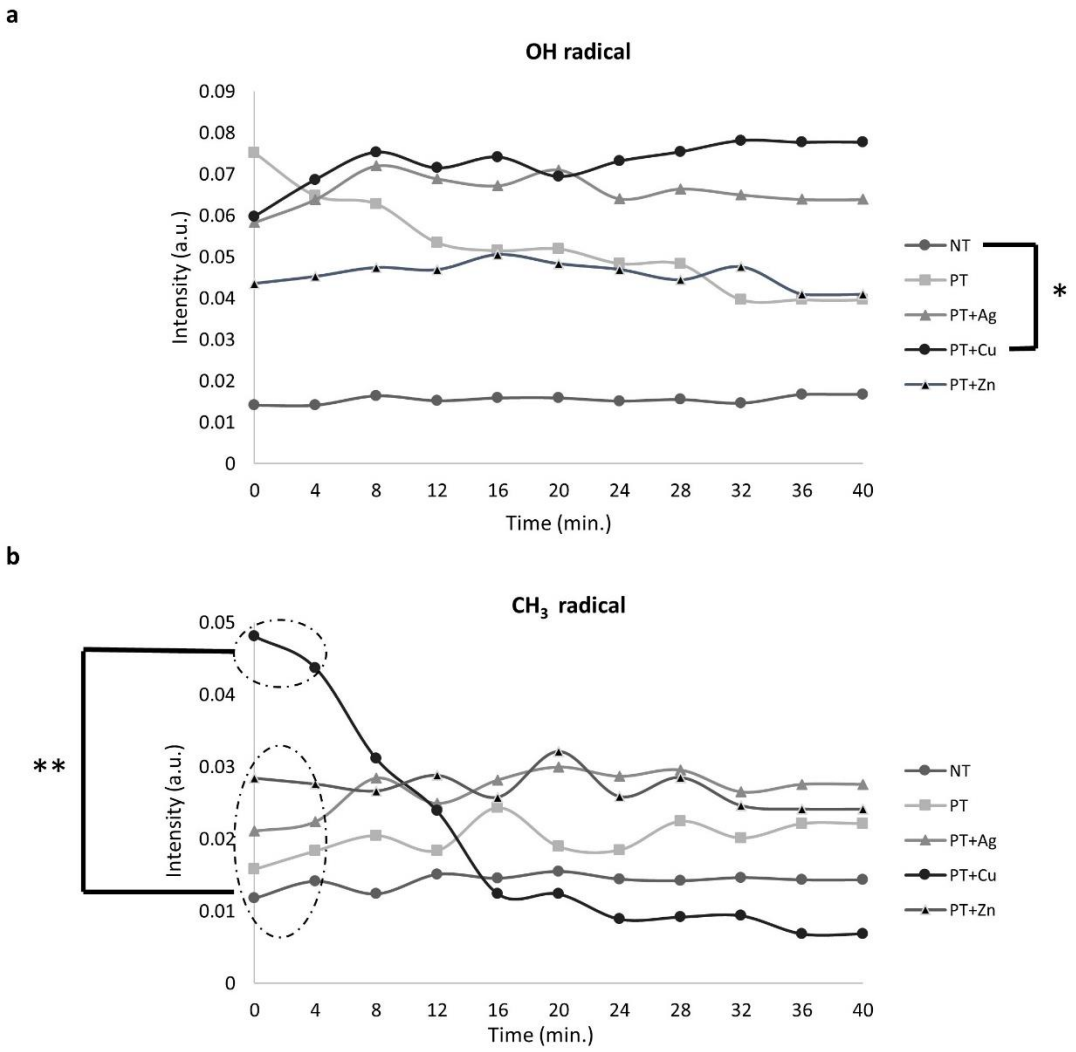

Figure 20. *Radical generation versus time plot of implants in 100 mM DMPO (n=3, *; p<0.05, **; p<0.01). a) ·OH radical, b) CH_3 radical.*

3.3.4.2 ROS generation of bacteria

To determine the generation of ROS from implants in presence of bacteria we first determined the formation of ROS by bacteria. Therefore, a scan of a NT implant - generating no radicals itself – was compared to a scan of a NT implant incubated with bacteria for 2 h (NT implant + adherent bacteria) and to a scan of bacteria only (**Figure 21**). The characteristic spectra of the ·OH and CH_3 radicals are shown as well. The NT implant shows no clear peaks, the NT implant + adherent bacteria shows clear peaks overlapping with both radicals and *S. aureus* shows peaks overlapping with the CH_3 radical. The NT implant + adherent bacteria differs significantly from the NT implant as well as from the bacteria in PBS.

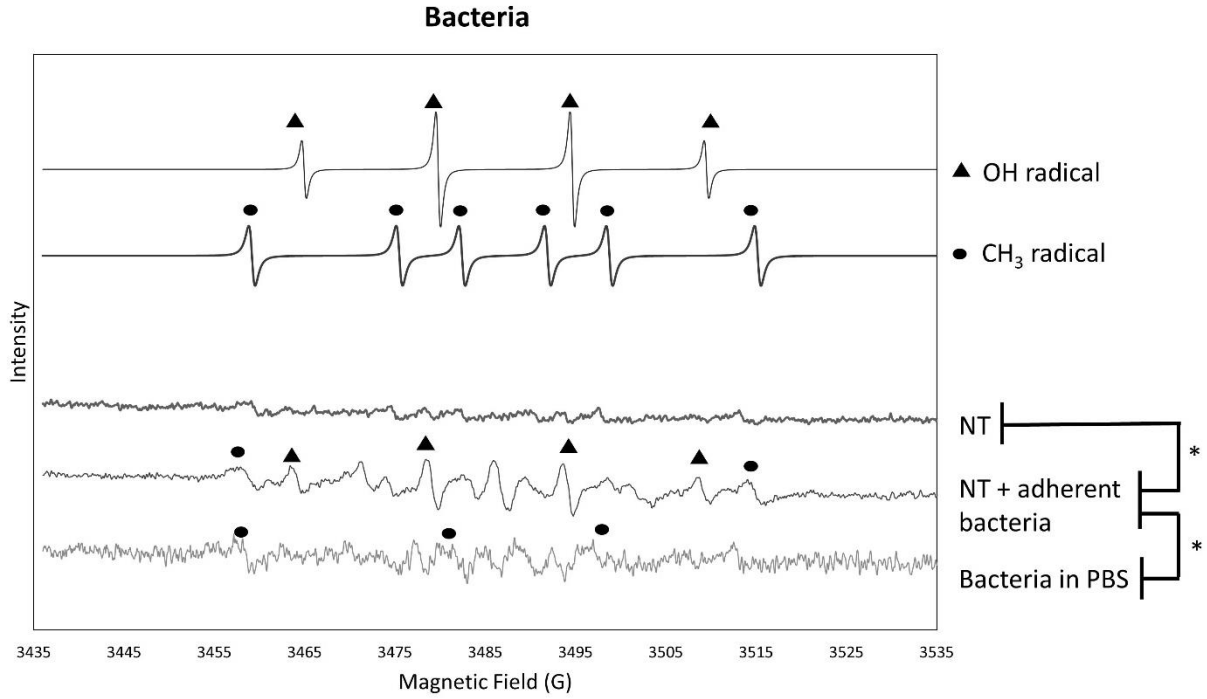

Figure 21. *ROS generation of bacteria (n=3, *; p<0.05, **; p<0.01). Top two lines represent characteristic spectra of the ·OH radical and the CH_3 radical (indicated by triangles and circles, respectively). Bottom three lines represent the average of 10 EPR spectra of (1) a NT implant, (2) a NT implant + adherent bacteria, and (3) bacteria in PBS.*

3.3.4.2 ROS generation of implants inoculated with bacteria

ROS generation of implants inoculated with *S. aureus* was performed using two methods, one examining the ROS generation of bacteria in PBS solution whereas the second method examines the ROS generation of the implant with adherent bacteria. The number of bacteria in PBS solution was 2×10^6 CFU whereas the number of adherent bacteria was counted per implant and is shown in **Figure 22**. The average of two counts[1] was taken since no significant differences between counts was observed (repeated measures ANOVA, p=0.873). **Figure 22** shows that bacteria adhere to all implants without significant differences between groups. The amount of adherent CFU is shown in **Figure 23b** as well. All PT implants in bacteria + PBS produce the ·OH radical (**Figure 23a**). However, PT+Cu shows the highest peaks and the average of all scans is significantly different from the NT implant (p=0.023). However, the repeated measures ANOVA indicated there are differences between scans considering groups (Shericity assumed of scans*group, p=0.006). It was observed that there are significant differences between NT and PT+Cu in all scans except scan 5 at t = 16 minutes (see **Figure 24a** where the data points of NT and PT+Cu are circled when significantly different)**.**

The implants with adherent bacteria show different results: no significant differences between groups was observed (**Figure 23b**). The repeated measures ANOVA indicated there is a significant difference between scans without considering the groups (Shericity assumed of scans, p=0.007). When considering the groups, no significant difference was observed between scans (p=0.254). Still, all scans were analysed separately resulting in the conclusion that no significant differences between groups was observed in each scan separately. However, when looking at **Figure 24b**, it can be concluded that all implants with adherent bacteria generate the ·OH radical. Surprisingly, PT+Cu shows less ROS generation when bacteria adhere compared to bacteria in solution. The opposite holds for PT, PT+Ag, and PT+Zn showing a higher ·OH generation when bacteria have adhered. However, for all biofunctionalized implant, no significant differences between implant only, implant + bacteria in PBS and adherent bacteria were observed (data shown in Appendix 9.5 **Figure 30**). The NT implant shows significant differences between implant only and implant + adherent bacteria (**Figure 21**). **Figure 30** in Appendix 9.5 shows the average spectra of each group separately in three situations: (1) ROS generation of the implant, (2) ROS generation of the implant with bacteria in PBS, (3) ROS generation of the implant with adherent bacteria.

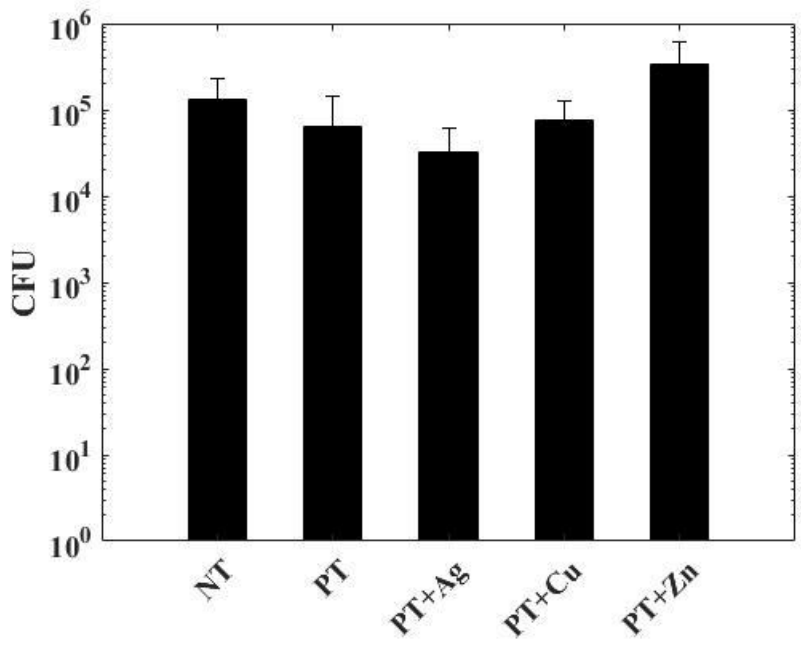

Figure 22. *Average of two counts of number of adherent bacteria (CFU) per implant group after 2 h of incubation (n=6).*

[1] EPR measurements of adherent bacteria were done three times whereas bacteria count was done twice.

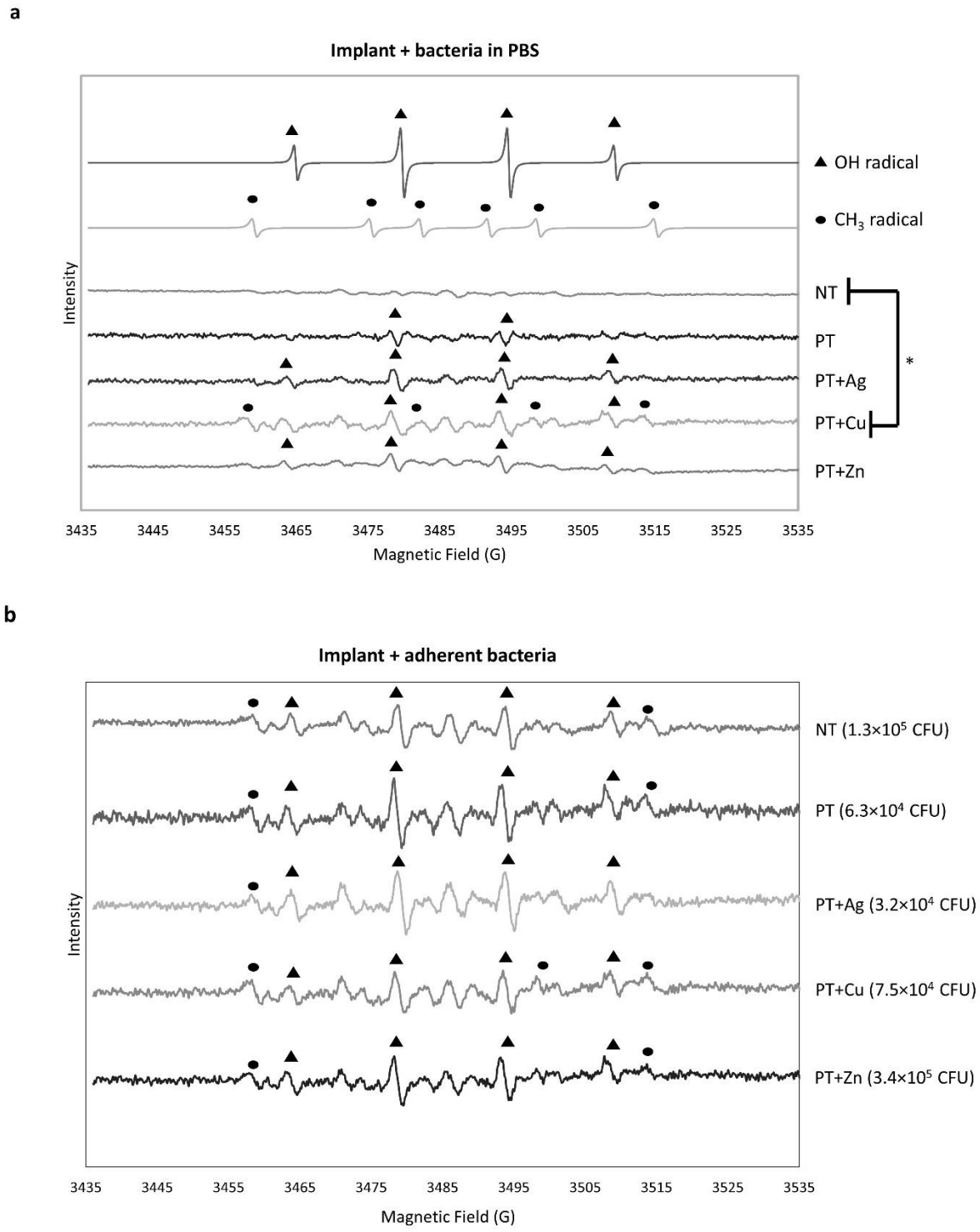

Figure 23. *ROS generation of implants inoculated with bacteria (n=3, *; p<0.05, **; p<0.01). Top two lines in a) represent characteristic spectra of the ·OH radical and the CH_3 radical (indicated by triangles and circles, respectively). Characterisation of the radicals on the implants is indicated by placing shapes (belonging to a certain radical) above each spectrum. Other lines represent the average of 10 EPR spectra in 100 mM DMPO of implants inoculated with bacteria.*
a) bacteria in PBS (~2×10^6 CFU), b) adherent bacteria after 2 h incubation.

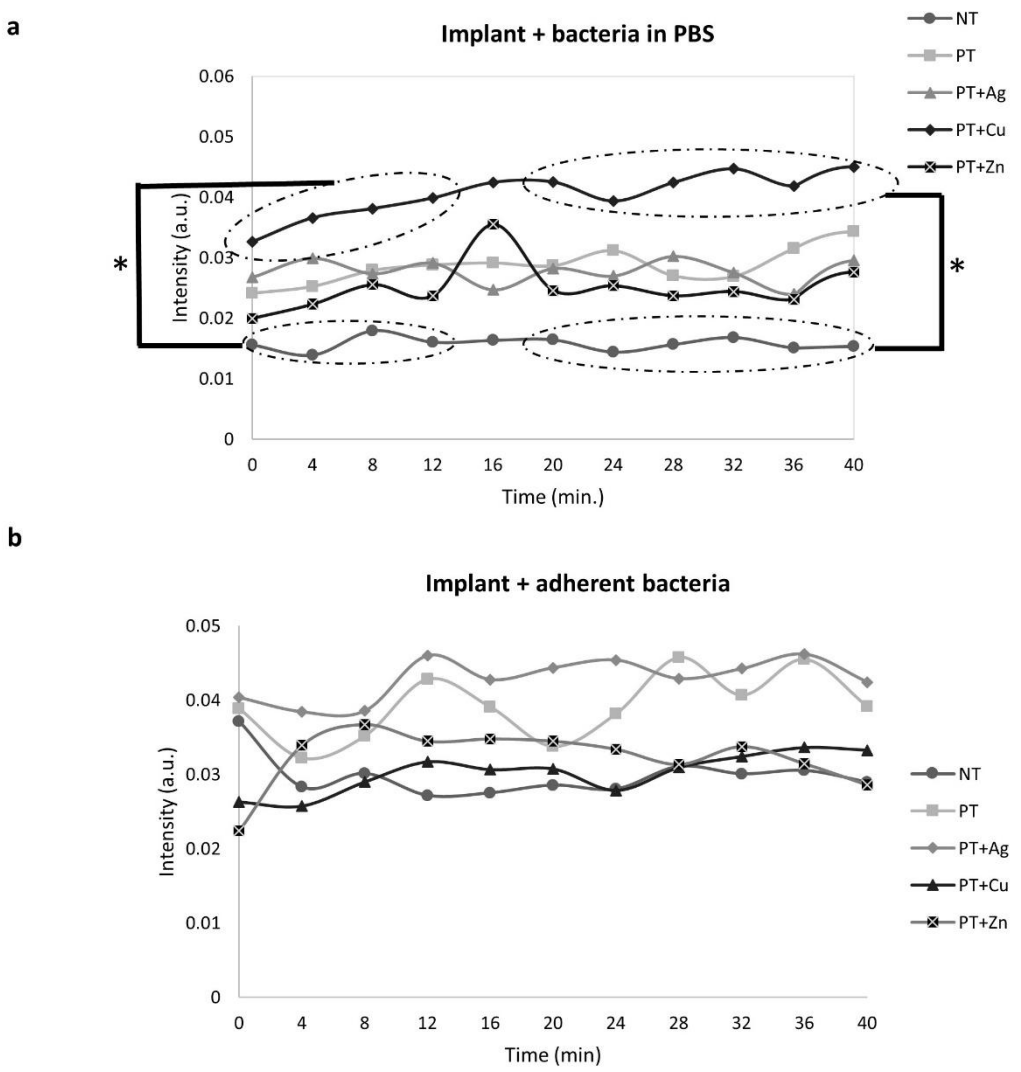

Figure 24. *·OH radical generation versus time plot in 100 mM DMPO (n=3, *; p<0.05, **; p<0.01) of a) implants with bacteria in PBS (~2×10^6 CFU), b) adherent bacteria after 2 h incubation.*

4 Discussion

This study aimed to correlate the antibacterial effects of Ag, Cu and Zn incorporated on titanium implants to its antibacterial mechanisms. SLM titanium implants were used [30] and treated by PEO, a process which incorporates the surface with an electrolyte containing Ca, Ca-GP, and metal NPs. After, the samples were tested on its antibacterial contact killing effects and ROS generation (**Figure 1**). Moreover, the antibacterial leaching effects of the implants were examined. Those results will be compared to the ion release profiles of the implants, of which the latter is known to be an antibacterial mechanism of Ag [31]–[33]. These results could be revealing which antibacterial mechanism plays a role in bacterial killing. This can be of great importance since knowing which antibacterial mechanism can improve further research on the antibacterial behaviour of the implants. Moreover, it will give insight in which direction further research should be going.

The synthesis of the TiO_2 surface on additively manufactured titanium implants (adapted from [30]) and the integration of the NPs was performed by PEO. During PEO, oxidation-reduction reactions induce thickening of the oxide layer on the titanium implants surface [34]. The growth of the oxide layers of all groups occurred in the first 10 ± 2 s for the discs and in the first 12 ± 2 s for the implants (**Figure 11 and 12**, respectively) after which the dielectric breakpoint appeared. At the dielectric breakpoint, the voltage has risen to a value sufficient for ionization to occur, seen as 'sparks'. For both implant and disc, the PT+Zn reached the highest voltage during the formation of the oxide layer (before dielectric breakpoint) and plasma discharging (after dielectric breakpoint). A potential cause for that can be that Zn was transformed to ZnO NPs having a slightly higher melting temperature. During plasma discharging or dielectric breakdown (in period time ±10-300 s), the electrolyte with the NPs can access the TiO_2 layer. The temperature rises resulting in the breakdown of water molecules. The resulting gases can be trapped in the layer resulting in pores on the surface of the discs and implants (**Figure 13**) [8] The similarities and differences between porous and solid surfaces are illustrated by **Figure 13**: they both show a PEO layer containing small holes. However, the porous implants also contain larger pores through which fluid can flow from one side to the other. Conversely, the pores created by PEO on solid discs are small: fluids cannot pass through, substantially different from porous implants. This difference will be of importance when testing direct contact killing.

After PEO, each PT group with NPs was visualized by SEM and analysed by EDS (**Figure 14**). To visualize NPs, magnifications higher than 8,000× should be reached. After, specific points can be chosen to analyse by EDS. For PT+Ag and PT+Cu, the elements Ag and Cu were easily found on the surface of the implants and their relative mass distribution was high (showing high peaks in the spectra in **Figure 14a and 14b**, respectively). This, however, was different for PT+Zn: finding the Zn NPs on the surface was rather difficult resulting in low peaks of the element Zn in the EDS analysis (**Figure 14c**). Yet, it is unlikely that Zn NPs did not stick to the surface, since the PEO settings were similar to the settings for PT+Ag and PT+Cu as well as the voltage-time transients (**Figure 11 and 12**). Besides, surfaces with bacterial adhesion were visualized for all groups (**Figure 16**). The implants were inoculated with bacteria (~2.5×10^4 CFU) for 2 h. All groups show bacterial adhesion, the initiation of forming a biofilm [2]. The results of SEM correspond to the direct contact results after 2 h (**Figure 18a**): all show bacterial adhesion; however, to the surfaces of NT, PT and PT+Zn implants more bacteria adhered (**Figure 16a, 16b, and 16e**, respectively).

The antibacterial effects as a result of direct contact killing (direct contact assay) and leaching (ZOI experiment) and the antibacterial mechanism of ROS generation of the metals incorporated on titanium implants were examined in this study. Furthermore, the ion release of the implants - another possible mechanism of action - can be found in Appendix 9.2 in **Figure 26 and 27**. The ZOI assay shows no antibacterial leaching effects for either Cu and Zn NPs, while the literature suggests otherwise [7], [35]–[40]. A cause for this lacking antibacterial effect can be that the minimum inhibitory concentration (MIC) of Cu and Zn incorporated on the implants is below the concentration of ion release of Cu and Zn. The MIC of Cu and Zn are approximately 10 and 1.25 mM, respectively (see **Figure 28 and 29** in Appendix 9.3). However, the ion release is equal to approximately 2100 ppb after 28 days (**Figure 27**

in Appendix 9.2). Rewriting units gives a value for the ion release of 0.033 mM for Cu and 0.032 mM for Zn (Appendix 9.4 for calculation) which is substantially lower than the MIC meaning that the ion release of Cu and Zn of the implants is not sufficient for bacterial killing. Comparing this to Ag - MIC of 0.002 mM which is lower than the ion release of the implant (0.0167 mM) - the results of **Figure 15** can be understood. As shown in Appendix 9.4, the concentration of Cu and Zn should be 302 times and 39 times as high before reaching the MIC meaning that a concentration of at least 117 g/L (3 g/L × 39) should be added to the PEO setup. This will not be possible. These results suggest that ion release is the antibacterial mechanism behind antibacterial leaching effects.

In addition to antibacterial leaching effects, direct contact killing properties were examined. Contact killing was examined by a direct contact assay, following the JIS standard [25] with an inoculum of 4×10^4 CFU for solid discs. Yet, there are limitations to this assay since it is impossible to conclude whether bacterial killing occurred as a result of solely contact killing. During the process, ions can be released, possibly contributing to bacterial killing. This causes a more complex interpretation of the results. However, this is the most accurate measure of contact killing since there is a clear contact area between bacteria and surface. **Figure 17a** shows that there are no significant differences between groups with a solid surface (inoculum equal to 4×10^4 CFU); therefore, an inoculum of 40 times as low (1×10^3 CFU) was chosen to conclude whether solid surfaces inhibited bacterial growth (**Figure 17b**). **Figure 17b** shows that the solid discs with Ag NPs do inhibit growth. Yet, the difference between PT+Ag and the other groups is not significant suggesting that solid PT surfaces do not show direct contact killing. A possible explanation can be that the concentration of the NPs stuck to the surface is not satisfactory for direct contact killing. The ion release of the solid surface was not examined. A suggestion for future work is, therefore, to print solid and porous surfaces with equal dimensions to compare the ion release and direct contact killing properties accurately.

The porous implants do show significant differences between groups (**Figure 18b**). **Figure 18b** shows that all biofunctionalized implants inhibit bacterial growth and are significantly different from a NT implant. Moreover, PT+Ag and PT+Cu implants counted 3 ± 8 CFU and 36 ± 55 CFU, respectively. However, both implant groups are not significantly different from PT (940 ± 765 CFU). A cause could be that the standard deviations (SD) of PT+Ag and PT+Cu are higher than the actual counted CFU. This high SDs can be a consequence of the fact that every implant is slightly different. The clamp (**Figure 5**) holds the implants close together. However, it was observed that it is difficult to create a closed surface, as is obtained with a solid disc. As a result, the bacterial solution can drip through the holes between the implants; subsequently, those bacteria cannot be killed by the NPs or adhere to the surface. If two samples of the same condition have a different space between the implants, the SD values will be high and the results, therefore, less trustworthy. This, again, can be solved by a porous surface as large as the discs.

Although the results show large deviations, there is a substantial difference with the results of the ZOI experiment. Particularly for the PT+Cu group as PT+Cu does not show a ZOI (**Figure 15**) whereas it shows clear antibacterial effects as a result of contact killing (**Figure 18b**). Hence, it can be concluded that PT+Cu implants (3 g/L of Cu NPs) do not show bacterial killing as a result of ion release but do show antibacterial effects as a result of contact killing. Furthermore, it is interesting to observe that contact killing in PT+Ag and PT+Cu started after 2 h of incubation (**Figure 18a**) since both groups show bacterial inhibition after this period, shown by the reduced amount of CFU. In summary, the porous implants show more bacterial killing than the solid discs. Contradictory theories were found in the literature suggesting that the pores of a porous implant can act as a hiding place against antimicrobial agents. Therefore, they suggest that porous implants have a higher infection rate than implants with a smooth surface before the invasion of human tissue [41]. However, after the invasion of human tissue, these hiding places will disappear as human tissue fills the pores and thereby the infection rate of porous implants is lower than for solid surfaces [41]. Oppositely, a theory by Zhaojun et al. (2016) suggested that the pores of an implant can act as a trap: bacteria are trapped into the pores of the implant and attacked by an ion or NP [10]. These theories, as well as the results of this study, let to **Figure 25**: the working surface area of a solid surface is smaller than a porous surface area (± 4 versus ± 25 cm), resulting in little space for NPs to adhere. However, a porous surface can act as a hiding place for bacteria. On the other hand, the pores of the implant can be used to trap bacteria. In conclusion, the contact killing results are contradictory to previous studies suggesting that Cu has best contact killing

properties, and Ag shows little contact killing properties [14]. A possible cause could be that PT+Ag shows antibacterial effects as a result of ion release instead of direct contact killing during the direct contact assay. **Figure 15** shows that PT+Ag is antibacterial, whereas PT+Cu is not. **Figure 18b** shows that PT+Cu does show contact killing. This, therefore, cannot be attributed to ion release since **Figure 15** showed that the concentration of Cu is not sufficient for ion release killing. Therefore, the antibacterial contact killing effects of PT+Cu can be fully attributed to contact killing and are not affected by ion release. This, in turn, is not the case for PT+Ag.

ROS generation – a possible antibacterial mechanism of contact killing [20] – was examined in this study. ROS can damage the cell membrane of the bacteria and thereby causing particles to move into the cell leading to cell death [42]. ROS generation was measured by EPR, a method which can detect specific radicals; the ·OH, CH_3, and $O_2^{\cdot-}$ radical. When DMPO reacts with ·OH and $O_2^{\cdot-}$ radicals, the adducts DMPO-OH and DMPO-OOH are formed, respectively [43], [44]. The DMPO-OOH adduct will then degrade into DMPO-OH, causing an overlap in their EPR spectra. This makes quantification of these radicals difficult· Therefore, the $O_2^{\cdot-}$ radical was only considered in ROS generation of the implants (**Figure 19**, rectangles) and disregarded in the other figures. Making a distinction between these radicals, a scavenger trapping one of them could be used in the future. Superoxide dismutase (SOD) can be used to trap $O_2^{\cdot-}$ and dimethyl sulfoxide (DMSO) for the ·OH radical [43].

ROS generation of the implants, bacteria, and implants inoculated with bacteria was examined (**Figure 8c**). All biofunctionalized implants generate the ·OH and CH_3 radical (**Figure 19**). Moreover, they all show a stable ·OH generation for 40 minutes (**Figure 20a**). However, there are differences between groups: a PT+Cu implant generates significantly more ·OH radical than a NT implant. This corresponds to the direct contact killing results, where PT+Cu shows contact killing (**Figure 18b**). PT+Ag also shows good contact killing properties; however, the ROS generation is not significantly different from a NT implant. It can, therefore, be assumed that the antibacterial effects of PT+Ag are predominantly caused by ion release. Additionally, the generation of the CH_3 radical is screened over time revealing that all groups except PT+Cu show a stable generation. PT+Cu shows the highest generation during the first 8 minutes (being significantly different from other groups) after which it decreases from 0.05 to 0 a.u. (**Figure 20b**). The CH_3 radical generation of PT+Cu can be an indication of its good direct contact killing properties, as suggested by Hans et al. (2016) [14]. Noteworthy is that all groups except NT show peaks which could not be attributed to a ROS; however, it is assumed they can be attributed to decay products of DMPO as it is possible that DMPO can react with the metals on the PT implants [45].

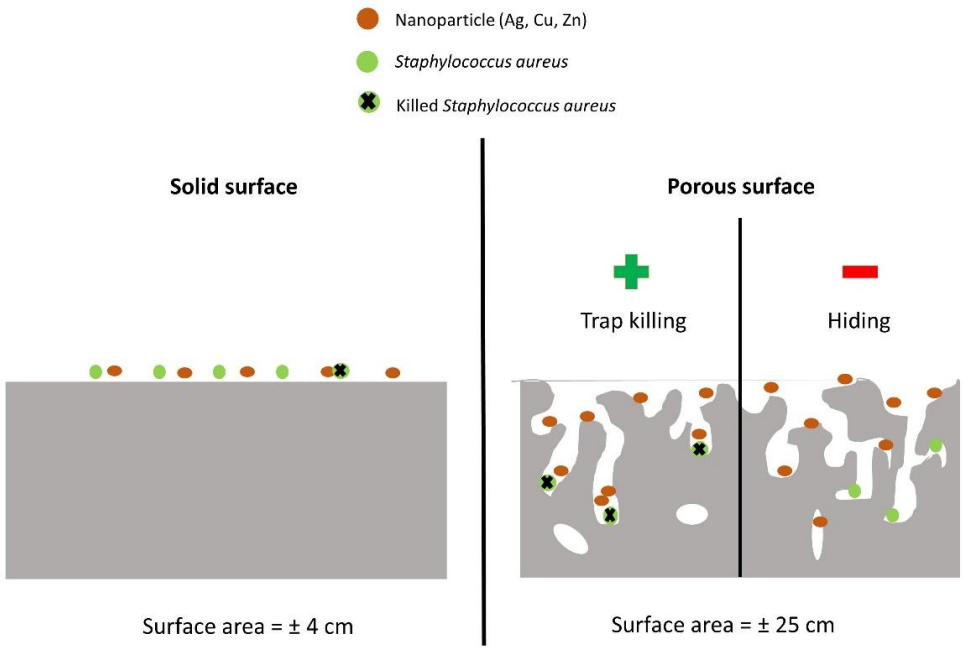

Figure 25. *Solid surfaces versus porous surfaces.*

Subsequently, the ROS generation of implants in contact with *S. aureus* was examined. This was done using two methods: the first examines ROS generation of bacteria in PBS and the second measures ROS generation of adherent bacteria. Both methods have limitations: during the process of the first method, it is unknown if and how many bacteria come into contact with the implant, whereas in the second method the ROS generation is not measured directly after contact between implant and bacteria. Yet, all biofunctionalized groups show less ROS generation when bacteria are added compared to implants only (**Figure 19** versus **Figure 23,** clearly illustrated in **Figure 30** in Appendix 9.5). This is contradictory to the results from Applerot et al. (2012, 2009): they suggested that the intensity of ROS increased when bacteria are added to a solution of Cu and Zn. They related the increase in ROS to bacterial killing for the reason that during the process of bacterial killing ROS can be formed [12], [46]. However, he did not test it on implants but rather on a solution with Cu or Zn. Moreover, studies on which method is best for measuring intracellular ROS are divergent: Samuni A. et al. (1989) was the first mentioning that DMPO was not sufficiently stable for examining ROS in cells [47]. Later, others also reported that DMPO can react with cellular components and is thereby not stable for measuring ROS [48], [49]. However, results from recent research show that DMPO is suitable for measuring intracellular ROS as it has low cytotoxicity and high accessibility to the cell [12], [46], [50]. It was, therefore, decided to proceed with measurements using DMPO.

Oppositely to biofunctionalized implants, the NT implant shows an increase in ROS generation (from 0.01 to 0.035 a.u.) when bacteria adhere. All biofunctionalized implants show ·OH radical generation when in contact with bacteria in PBS (**Figure 23a**). Again, a PT+Cu implant is significantly different from a NT implant. However, there is a time dependence meaning that the ·OH radical generation is not stable for 40 minutes in all groups. **Figure 24a** shows that a PT+Cu and NT implant are not significantly different at t = 16 minutes. An explanation for the unstable ·OH generation can be that the number of bacteria in contact with the implant differs over time. The second method for testing ROS generation of implants with bacteria was inoculation with bacteria (~6×10^6 CFU) and 2 h incubation, similar to the direct contact assay for 2 h (**Figure 18a**). It would, therefore, be expected that PT+Ag and PT+Cu would generate most ROS since they show bacterial inhibition after 2 h. For implants only, this was observed since a PT+Cu implant shows significantly more ·OH radical than a NT implant (**Figure 19 and 20a**). However, this correlation cannot be made for implants with adherent bacteria since no significant differences between groups were observed (**Figure 24b**). This, however, can also be a consequence of the fact that PT+Ag and PT+Cu have already killed bacteria within the 2 h incubation, resulting in a lower amount of CFU present on the implant, causing lower ROS generation.

5 Conclusion

Titanium implants became biofunctionalized by the process of PEO. Besides, PEO enabled adherence of the metal NPs Ag, Cu, and Zn. PT+Ag showed best *in vitro* antibacterial leaching effects which can be attributed to the ion release of Ag^+ as well as the low MIC for bacterial killing. In addition to the antibacterial leaching effects, it was concluded that all PT porous implants show significant differences with the NT porous implant in direct contact killing after 24 h of incubation. Furthermore, the antibacterial mechanism of ROS generation was examined. It can be concluded that a PT+Cu implant is significantly different from a NT implant in terms of ·OH generation with and without the presence of bacteria in PBS. It is, therefore, assumed that the contact killing properties of Cu can be linked to the ROS generation of a PT+Cu implant. The significant differences in contact killing properties between groups, however, was not observed for the direct contact killing properties of solid surfaces. Hence, the porous surfaces show better contact killing properties than the solid discs. Furthermore, ROS generation was expected to increase when examining implants inoculated with *S. aureus* since bacteria itself can produce ROS. Oppositely, it was observed that ROS generation decreased after implants came into contact with bacteria (in PBS or adherent). In summary, ion release of Ag^+ could be linked to the antibacterial leaching effects. Besides, a correlation between ROS generation and contact killing is suggested for porous titanium implants bearing Cu NPs.

6 Acknowledgements

I would like to thank Dr. Ir. Iulian Apachitei for being my supervisor during this project. I always felt like I could walk into his office for help. Throughout the whole year, I had a daily supervisor Ir. Ingmar van Hengel which guided me through the whole project. I felt like I could ask all (stupid) questions, which made me feel comfortable. They both helped me to learn doing good research and by improving my writing skills. Ingmar also learned me how to use SEM and made me familiar in the lab at the UMC Utrecht.

Also, I would like to thank Sander Leeflang for his technical assistance in the PEO-lab, Wim Velt for his assistance in building the clamp, Dr. Ir. Peter-Leon Hagedoorn and Ir. Hongshan San for their assistance at the EPR room, Ir. Khashayar Modaresifar for preparing bacterial cultures for EPR and helping me in the HTS lab, Prof. Ad Fluit for his hospitality at the UMC Utrecht, Melissa Tierolf for her assistance at the UMC Utrecht, and Ir. Niko Eka Putra for his help with the data acquisition of EPR spectra.

7 Abbreviations

Ag	=	Silver
BHI	=	Brain heart infusion
CA	=	Calcium acetate
Ca-GP	=	Calcium glycerophosphate
CFU	=	Colony forming units
CH_3	=	Methyl
Cu	=	Copper
DIP	=	Distal phalangeal
DMPO	=	5,5-dimethyl-pyrroline N-oxide
DMSO	=	dimethyl sulfoxide
EDS	=	Energy dispersive x-ray spectroscopy
EPR	=	Electron paramagnetic resonance
ICP-MS	=	Inductively coupled plasma mass spectroscopy
IAI	=	Implant associated infection
MRSA	=	Methicillin resistant *Staphylococcus aureus*
NP	=	Nanoparticle
NT	=	Non-treated
$O_2^{\cdot -}$	=	Superoxide
OA	=	Osteoarthritis
OD	=	Optical density
·OH	=	Hydroxyl
OP	=	Osteoporosis
PBS	=	Phosphate buffered saline
PEO	=	Plasma electrolytic oxidation
PT	=	PEO-treated
ROS	=	Reactive oxygen species
SEM	=	Scanning electron microscopy
SLM	=	Selective laser melting
SOD	=	Superoxide dismutase
THR	=	Total hip replacement
TSB	=	Tryptic soy broth
Zn	=	Zinc
ZOI	=	Zone of inhibition

8 References

[1] E. M. Hetrick and M. H. Schoenfisch, “Reducing implant-related infections: active release strategies,” *Chem. Soc. Rev.*, vol. 35, no. 9, p. 780, Aug. 2006.

[2] L. G. Harris and R. G. Richards, “Staphylococci and implant surfaces: a review,” *Injury*, 2006.

[3] M. Cross, E. Smith, D. Hoy, and S. Nolte, “The global burden of hip and knee osteoarthritis: estimates from the Global Burden of Disease 2010 study,” *Clin. Epidemiol. Res.*, vol. 73, no. 7, pp. 1323–1330, 2014.

[4] C. R. Arciola, D. Campoccia, and L. Montanaro, “Implant infections: Adhesion, biofilm formation and immune evasion,” *Nat. Rev. Microbiol.*, vol. 16, no. 7, pp. 397–409, 2018.

[5] G. Laverty, S. P. Gorman, and B. F. Gilmore, “Biomolecular mechanisms of staphylococcal biofilm formation,” *Future Microbiol.*, vol. 8, no. 4, pp. 509–524, 2013.

[6] J. Raphel, M. Holodniy, S. B. Goodman, and S. C. Heilshorn, “Biomaterials Multifunctional coatings to simultaneously promote osseointegration and prevent infection of orthopaedic implants,” *Biomaterials*, vol. 84, pp. 301–314, 2016.

[7] S. Ferraris and S. Spriano, “Antibacterial titanium surfaces for medical implants,” *Mater. Sci. Eng. C*, vol. 61, pp. 965–978, 2016.

[8] A. L. Yerokhin, X. Nie, A. Leyland, A. Matthews, and S. J. Dowey, “Plasma electrolysis for surface engineering,” vol. 122, pp. 73–93, 1999.

[9] R. M. Grotenhuis, “Antibacterial mechanisms of silver, copper and zinc and their detection methods,” TU Delft, 2019.

[10] Z. Jia *et al.*, “Bioinspired anchoring AgNPs onto micro-nanoporous TiO2 orthopedic coatings: Trap-killing of bacteria, surface-regulated osteoblast functions and host responses,” *Biomaterials*, vol. 75, pp. 203–222, 2016.

[11] M. A. F. Afzal, S. Kalmodia, P. Kesarwani, B. Basu, and K. Balani, “Bactericidal effect of silver-reinforced carbon nanotube and hydroxyapatite composites,” *J. Biomater. Appl.*, vol. 27, no. 8, pp. 967–978, 2013.

[12] G. Applerot *et al.*, “Understanding the antibacterial mechanism of CuO nanoparticles: Revealing the route of induced oxidative stress,” *Small*, vol. 8, no. 21, pp. 3326–3337, 2012.

[13] G. Applerot, J. Lellouche, N. Perkas, Y. Nitzan, A. Gedanken, and E. Banin, “ZnO nanoparticle-coated surfaces inhibit bacterial biofilm formation and increase antibiotic susceptibility,” *RSC Adv.*, vol. 2, no. 6, pp. 2314–2321, 2012.

[14] M. Hans, S. Mathews, F. Mücklich, and M. Solioz, “Physicochemical properties of copper important for its antibacterial activity and development of a unified model,” *Biointerphases*, vol. 11, no. 1, p. 018902, 2016.

[15] M. Hans, A. Erbe, S. Mathews, Y. Chen, M. Solioz, and F. Mücklich, “Role of copper oxides in contact killing of bacteria,” *Langmuir*, vol. 29, no. 52, pp. 16160–16166, 2013.

[16] S. Mathews, M. Hans, F. Mücklich, and M. Solioz, “Contact killing of bacteria on copper is suppressed if bacterial-metal contact is prevented and is induced on iron by copper ions,” *Appl. Environ. Microbiol.*, vol. 79, no. 8, pp. 2605–2611, 2013.

[17] I. A. J. Van Hengel *et al.*, “Selective laser melting porous metallic implants with immobilized silver nanoparticles kill and prevent biofilm formation by methicillin-resistant Staphylococcus aureus,” *Biomaterials*, 2017.

[18] B. Necula, “Silver-based antibacterial surfaces for bone implants,” TU Delft, 2013.

[19] K. Unfried, C. Albrecht, L. O. Klotz, A. Von Mikecz, S. Grether-Beck, and R. P. F. Schins, “Cellular responses to nanoparticles: Target structures and mechanisms,” *Nanotoxicology*, vol. 1, no. 1, pp. 52–71, 2007.

[20] M. Vincent, R. E. Duval, P. Hartemann, and M. Engels-Deutsch, “Contact killing and antimicrobial properties of copper,” *J. Appl. Microbiol.*, vol. 124, no. 5, pp. 1032–1046, 2018.

[21] C. E. Santo *et al.*, “Bacterial Killing by Dry Metallic Copper Surfaces,” vol. 77, no. 3, pp. 794–802, 2011.

[22] M. J. Davies, “Detection and characterisation of radicals using electron paramagnetic resonance (EPR) spin trapping and related methods,” *Methods*, vol. 109, pp. 21–30, 2016.

[23] A. B. Bauer, D. M. Perry, and W. M. Kirby, “Single-disk antibiotic-sensitivity testing of staphylococci: An analysis of technique and results,” *AMA Arch. Intern. Med.*, vol. 104, no. 2, pp. 208–216, 1959.

[24] M. Tierolf, “Antibacterial Surface Bearing Nanoparticles on Additive Manufactured Titanium Implants,” Delft, 2018.

[25] J. I. Standard, “Jis z 2801 :2000,” vol. 2000, 2000.

[26] D. T. Petatis and M. P. Hendrich, “Quantitative interpretation of multifrequency multimode EPR spectra of metal containing proteins, enzymes, and biomimetic complexes,” *Methods Enzymol.*, vol. 563, pp. 171–208, 2015.

[27] W. Freinbichler *et al.*, “Highly reactive oxygen species: Detection, formation, and possible functions,” *Cell. Mol. Life Sci.*, vol. 68, no. 12, pp. 2067–2079, 2011.

[28] T. (Bruker B. Ralph, “Xenon User’s Guide,” 2011.

[29] G. R. Bueyrner, G. S. F. Forschungszentrum, and S. D. Neuhcrberg, “SPIN TRAPPING : ESR PARAMETERS OF SPIN ADDUCTS *,” vol. 3, pp. 259–303, 1987.

[30] I. van Hengel, “Additively manufactured selfdefending bone implants to prevent implant-associated infection,” TU Delft, 2016.

[31] N. Durán, M. Durán, M. B. de Jesus, A. B. Seabra, W. J. Fávaro, and G. Nakazato, “Silver nanoparticles: A new view on mechanistic aspects on antimicrobial activity,” *Nanomedicine Nanotechnology, Biol. Med.*, vol. 12, no. 3, pp. 789–799, 2016.

[32] S. Prabhu and E. K. Poulose, “Silver nanoparticles: mechanism of antimicrobial action, synthesis, medical applications, and toxicity effects,” *Int. Nano Lett.*, vol. 2, no. 1, p. 32, 2012.

[33] T. C. Dakal, A. Kumar, R. S. Majumdar, and V. Yadav, “Mechanistic basis of antimicrobial actions of silver nanoparticles,” *Front. Microbiol.*, vol. 7, no. NOV, pp. 1–17, 2016.

[34] A. L. Yerokhin, X. Nie, A. Leyland, and A. Matthews, “Characterisation of oxide films produced by plasma electrolytic oxidation of a Ti–6Al–4V alloy,” *Surf. Coatings Technol.*, vol. 130, no. 2–3, pp. 195–206, Aug. 2000.

[35] L. Fowler, O. Janson, H. Engqvist, S. Norgren, and C. Öhman-Mägi, “Antibacterial investigation of titanium-copper alloys using luminescent Staphylococcus epidermidis in a direct contact test,” *Mater. Sci. Eng. C*, vol. 97, no. December 2018, pp. 707–714, 2018.

[36] K. Sunada, T. Watanabe, and K. Hashimoto, “Bactericidal Activity of Copper-Deposited TiO 2 Thin Film under Weak UV Light Illumination,” *Environ. Sci. Technol.*, vol. 37, pp. 4785–4789, 2003.

[37] Q. Du *et al.*, “The hydrothermal treated Zn-incorporated titania based microarc oxidation coating: Surface characteristics, apatite-inducing ability and antibacterial ability,” *Surf. Coatings Technol.*, vol. 352, no. 2, pp. 489–500, 2018.

[38] H. Hu, W. Zhang, Y. Qiao, X. Jiang, X. Liu, and C. Ding, “Antibacterial activity and increased bone marrow stem cell functions of Zn-incorporated TiO2coatings on titanium,” *Acta Biomater.*, vol. 8, no. 2, pp. 904–915, 2012.

[39] R. Hong, T. Y. Kang, C. A. Michels, and N. Gadura, “Membrane lipid peroxidation in copper alloy-mediated contact killing of Escherichia coli,” *Appl. Environ. Microbiol.*, vol. 78, no. 6, pp. 1776–1784, 2012.

[40] P. Huang *et al.*, “Enhanced antibacterial activity and biocompatibility of zinc-incorporated organic-inorganic nanocomposite coatings via electrophoretic deposition,” *Colloids Surfaces B Biointerfaces*, vol. 160, pp. 628–638, 2017.

[41] K. Merritt and J. W. Shafer, “Implant Site Infection Rates with Porous and Dense Materials *,” vol. 13, no. April 1976, pp. 101–108.

[42] M. Li, J. Yin, W. G. Wamer, and Y. M. Lo, “Mechanistic characterization of titanium dioxide nanoparticle-induced toxicity using electron spin,” *J. Food Drug Anal.*, vol. 22, no. 1, pp. 76–85, 2014.

[43] Bruker Biospin, “EPR Detection of the Superoxide Free Radical with the Nitrone Spin Traps DMPO and BMPO.”

[44] J.-L. Clément, N. Ferré, D. Siri, H. Karoui, A. Rockenbauer, and P. Tordo, “Assignment of the EPR Spectrum of 5,5-Dimethyl-1-pyrroline *N* -Oxide (DMPO) Superoxide Spin Adduct †,” *J. Org. Chem.*, vol. 70, no. 4, pp. 1198–1203, Feb. 2005.

[45] G. R. Buettner, “The spin trapping of superoxide and hydroxyl free radicals with DMPO (5,5-dimethylpyrroline-N-oxide): more about iron.,” *Free Radic. Res. Commun.*, vol. 19 Suppl 1, no. 0 1, pp. S79-87, 1993.

[46] G. Applerot *et al.*, “Enhanced Antibacterial Activity of Nanocrystalline ZnO Due to Increased ROS-Mediated Cell Injury,” *Adv. Funct. Mater.*, vol. 19, no. 6, pp. 842–852, Mar. 2009.

[47] A. Samuni, A. Samuni, and H. M. Swartz, “The cellular-induced decay of DMPO spin adducts of ·OH and ·O2−,” *Free Radic. Biol. Med.*, vol. 6, no. 2, pp. 179–183, Jan. 1989.

[48] N. Khan *et al.*, “Spin traps: in vitro toxicity and stability of radical adducts,” *Free Radic. Biol. Med.*, vol. 34, no. 11, pp. 1473–1481, Jun. 2003.

[49] S. I. Dikalov and D. G. Harrison, “Methods for Detection of Mitochondrial and Cellular Reactive Oxygen Species,” *Antioxid. Redox Signal.*, vol. 20, no. 2, pp. 372–382, Jan. 2014.

[50] S. Venkataraman, I. Alimova, R. Fan, P. Harris, N. Foreman, and R. Vibhakar, “MicroRNA 128a Increases Intracellular ROS Level by Targeting Bmi-1 and Inhibits Medulloblastoma Cancer Cell Growth by Promoting Senescence,” *PLoS One*, vol. 5, no. 6, p. e10748, Jun. 2010.

[51] N. E. Putra, “Antibacterial Surfaces Bearing Silver and Zinc Nanoparticles on Additively Manufactured Titanium Implants,” TU Delft, 2018.

[52] V. Valerio, “Antibacterial silver- and copper-based surfaces on additively manufactured titanium implants,” TU Delft, 2018.

9 Appendix

9.1 EDS mass percentages per NP

Table 5. *Mass and atom percentages of NPs in EDS analysis.*

Metal NP	Mass %	Atom %
Ag	14.38	3.13
Cu	27.21	11.12
Zn	3.92	2.39

9.2 Results ion release

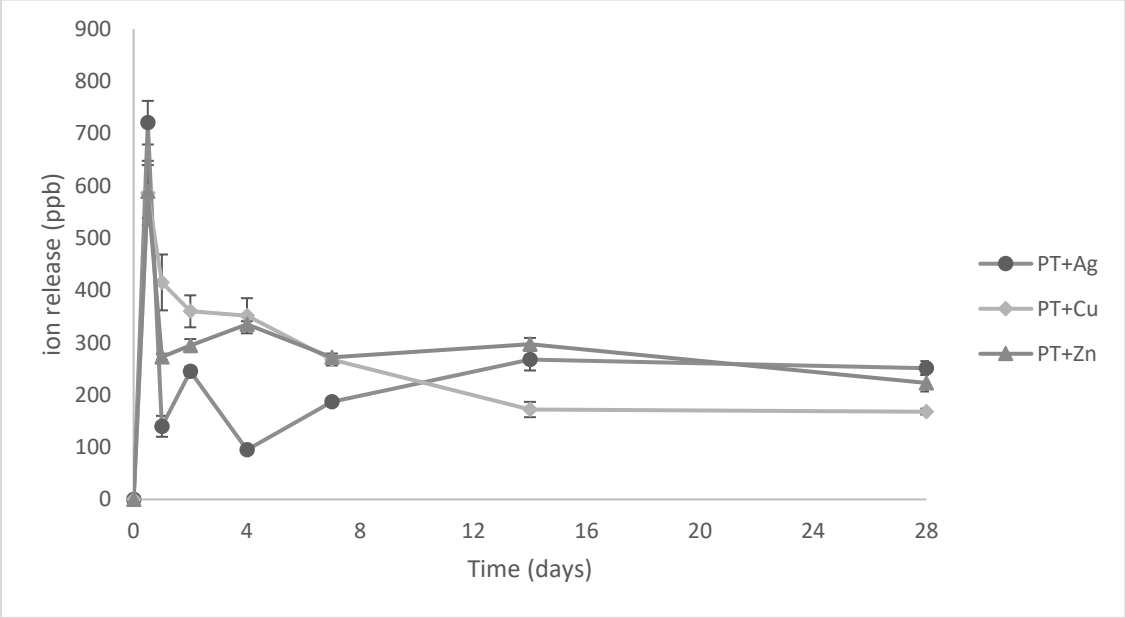

Figure 26. *Non-cumulative ion release results (n=3). Adapted from* [51].

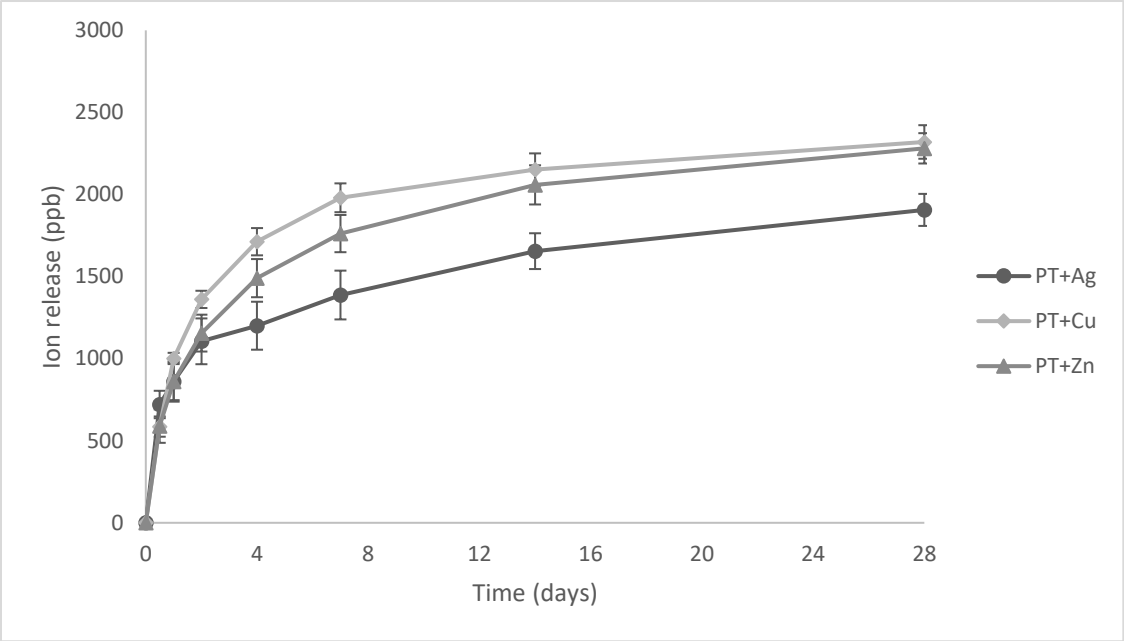

Figure 27. *Cumulative ion release results (n=3). Adapted from* [52]

9.3 MIC results

Figure 28. *MIC results of $AgNO_3$ and $Cu(NO_3)_2$. Adapted from* [24].

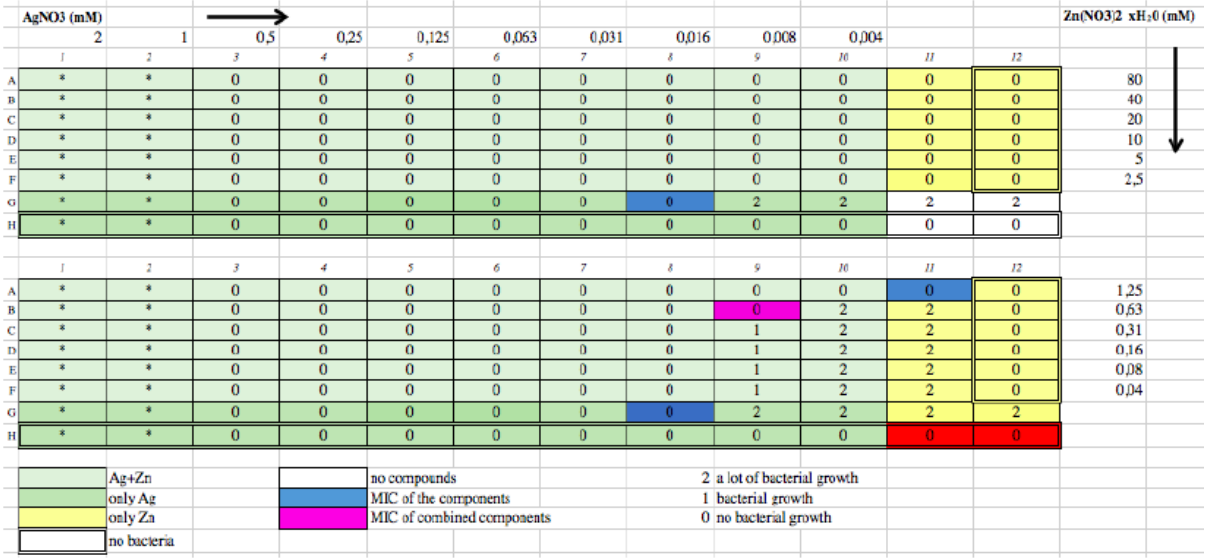

Figure 29. *MIC results of $AgNO_3$ and $Zn(NO_3)_2$. Adapted from* [24].

9.4 Calculation ppb to mM

Ag

Ion release is 1800 ppb = 2 g/m^3

Molar mass Ag = 107.87 g/mole

MIC is in units mM : [mM] = [mole/m^3]

$$\frac{\frac{g}{m^3}}{\frac{g}{mole}} = \frac{g}{m^3} \times \frac{mole}{g} = \frac{g \times mole}{m^3 \times g} = \frac{mole}{m^3}$$

So, for Ag 1800 ppb is equal to a 1.8/107.87=0.0167 mM

Sufficient since MIC for Ag is 0.002 mM.

Cu

Ion release is 2100 ppb = 2.1 g/m^3

Molar mass Cu = 63.546 g/mole

For Cu 2100 ppb is equal to 2.1/63.546=0.033 mM

The MIC of Cu is 10 mM, so the concentration of Cu should be 10/0.033 = 302 times as large as it is now.

Zn

Ion release is 2100 ppb = 2.1 g/m^3

Molar mass Zn = 65.38 g/mole

For Zn 2100 ppb is equal to 2.1/65.38=0.032 mM

The MIC of Zn is 1.25 mM, so the concentration of Zn should be 1.25/0.032 = 39 times as large as it is now.

9.5 Results EPR per group

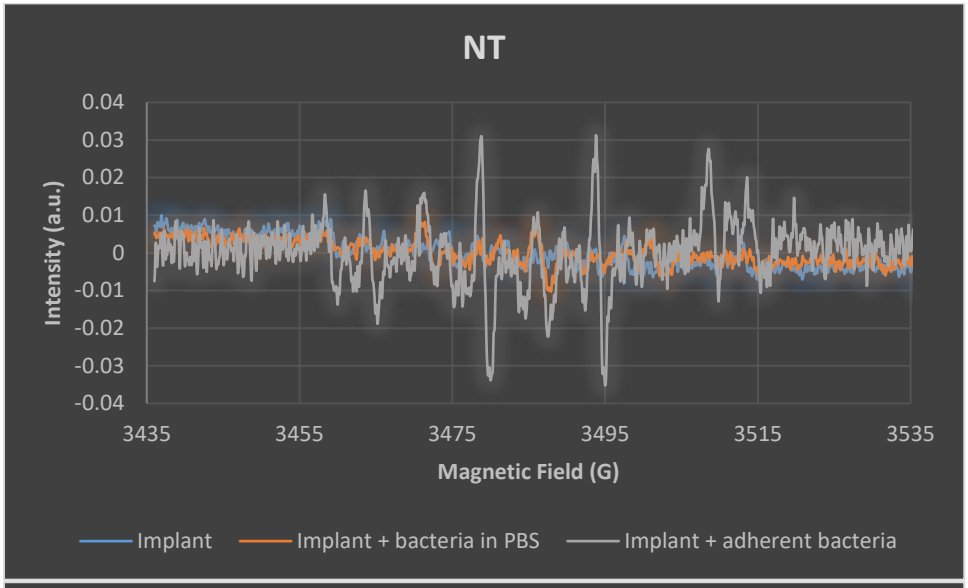

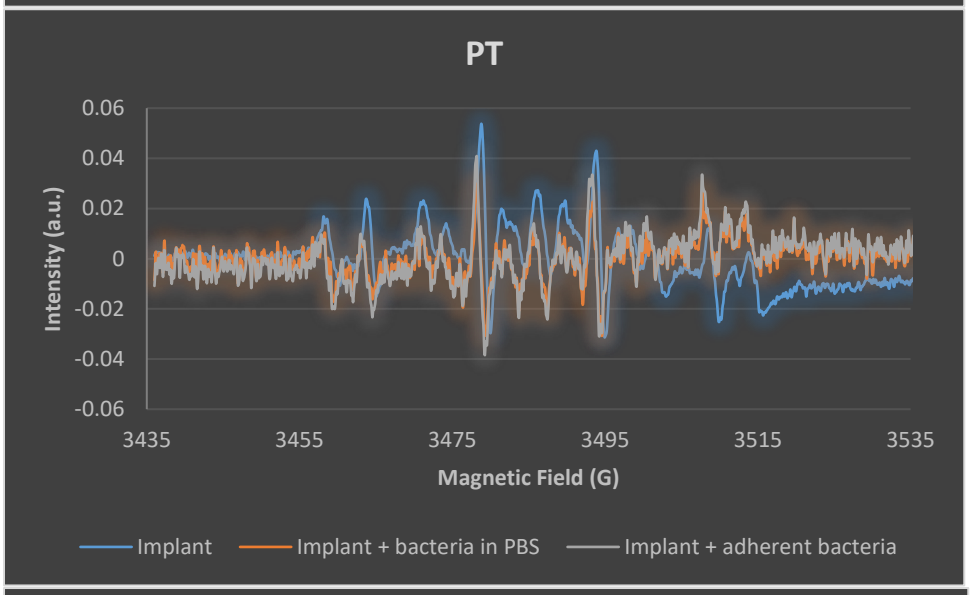

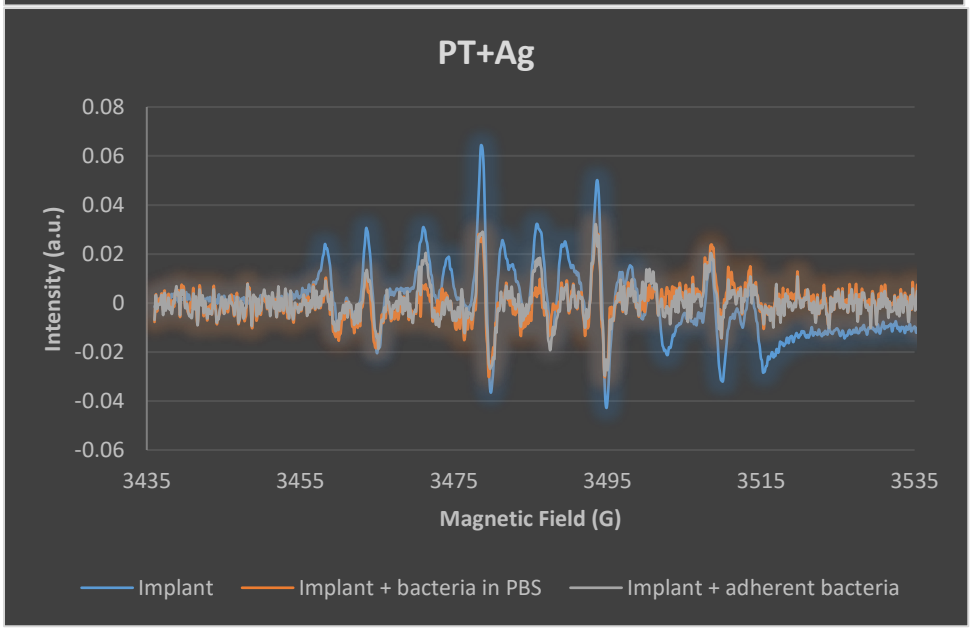

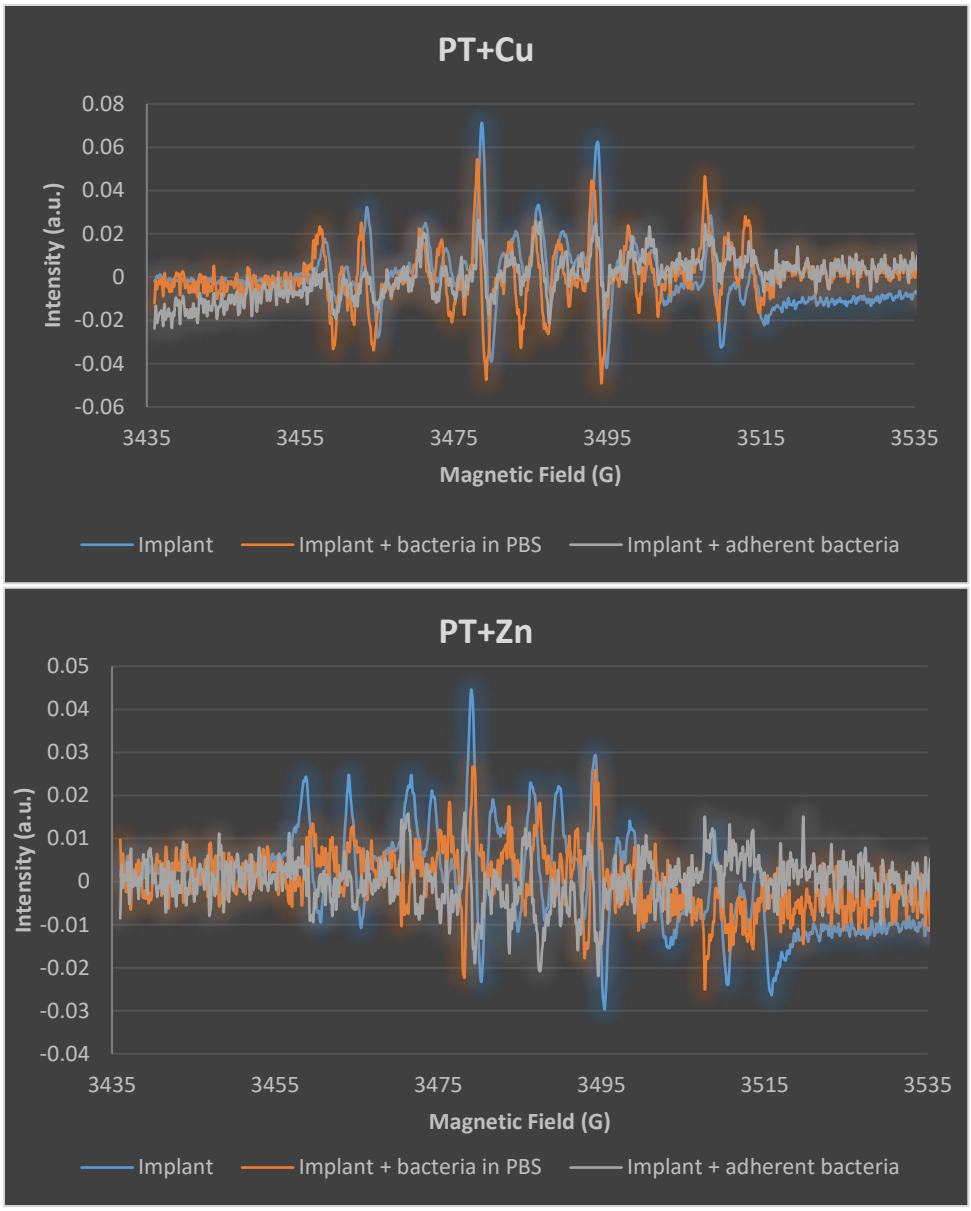

Figure 30. *EPR results per group in three situations (n=3): (1) ROS generation of implant, (2) ROS generation of implant with bacteria in PBS, (3) ROS generation of implant with adherent bacteria.*

9.6 Protocols

Protocol 1: Plasma Electrolytic Oxidation

18sep2018

Aim. To synthesis TiO_2 layers enriched with calcium and phosphorus (with antibacterial NPs i.e. nanoparticles) on titanium substrate.

Procedure

Preparation for experiment

1. **Turn on cooling system for beaker (NOTE: will take some time)**
   - Turn on lower and higher button thermostatic bath *(= left of PEO beaker and had one small device with temperature settings and one big which says :'do not wet')*
   - Turn on stirring device and set temperature of the device to 0 °C (upper right corner) and rotation to 500 rpm. *(= PEO device. Both turning wheels should be used to set temperature and stirring)*

2. **Electrolyte preparation**
   - Prepare 19.2g (24 g/L) calcium acetate and 3.36g (4.2 g/L) calcium glycerophosphate in 800 ml demineralized water. (*Use Erlenmeyer. First put in powders with filter and then 800 ml demirelazid water to pour leftover powders in)*
   - Stir until the solution is 'clear' and the acetate and glycerophospate is dissolved homogenously. (*Use other stirrer)*
   - Pour 800 mL of the electrolyte into PEO beaker and stir at 500 rpm.
     ⇒ Note: electrolyte preparation with NPs requires additional step first (see 3.)
   - Cool down the electrolyte until the temperature is below 10 °C.
   - Store in fridge with name and date (max. up to 2 weeks).

3. **Electrolyte preparation with nanoparticles (NPs).**
   - Pour 700 mL electrolyte (room temperature) in beaker glass)
   - Add **slowly** 3 g/L NPs into 700 mL electrolyte, i.e. 2.4 g for 800 mL electrolyte.
   - Stir between 500-700 rpm (electrolyte with NPs will become 'troebel').
   - Sonicate 2 x 5 minutes, stir for 5 minutes in between.
   - Pour 700 mL of the electrolyte into PEO beaker.
   - Use the left over (circa 100 mL) electrolyte to rinse the beaker glass, sonicate and pour the remaining in the PEO beaker.
   - Put thermometer in beaker glass
   - Stir at 500 rpm and cool down the electrolyte until the temperature is below 10 °C

4. **Cathode preparation**
   - Stainless steel cathode was stored in 50% sulfuric acid (50% sulf acided and 50% demineralized water).
   - Put the cathode inside beaker glass and clean it with running tap water for 5 minutes.
   - Clean the cathode with demineralized water (rinse the inside and the outside of the cathode twice)
   - Insert the cathode into PEO beaker and **do not forget** to secure the wire of the cathode to the tripod.

5. **Preparation of non-treated samples (NT)**
    - Sonicate as-manufactured samples in acetone for 5 minutes (use a stopwatch).
    - Sonicate samples in 96% ethanol for 5 minutes.
    - Sonicate samples in demineralized water for 5 minutes.
    - Dry samples.

NOTE: the amount of liquids used must be sufficient such that the samples are 'under water'
The steps above can be done before PEO experiment, so that clean samples are ready to be used during PEO experiment.

- Clip a small part on the samples with crocodile clippers (approx. 3 cm remaining of the sample)
- Seal the clippers properly with waterproof tape (tape 3 times)

6. **Turn on PEO device**
    - Turn on power supply (*ACS – Power source)*
    - Turn on oscillator (*Tektronix)*
    - Turn on interface (*National instruments*)

NOTE: Turn off in reversed order!

7. **Software**
    - Start up the computer present in the lab and to get access fill in the password: *biolab1*.
    - Open the program **Acquisition**
        - ⇒ Open Acquire → Choose file → D: **own file (FILE NAME)** → Select current derivative.
        - ⇒ Set Y-axis from 0 to 300 Voltage
        - ⇒ Open the program **Measurement & Automation**
        - ⇒ Device and Interfaces → NI-DAQX... → NI-SCXI → Right-click → Reset chassis.

8. **Set current**
    - Place a **previously oxidized sample** into the electrolyte and measure the temperature (between 5-8 °C , ≤ 6°C).
    - Connect the electronic cables, *black cable* for cathode and *red cable* for anode.
    - Press VAC button
    - Press load button → turns green.
    - Use buttons on the right of the device to reach desired current
        - ⇒ Require current density is 20 A/dm^2 ≈ 389 mA for 1 sample
        - ⇒ 4 samples ≈ 1556 mA ≈ 1.556 A
        - ⇒ For discs: 2.543 A
    - Turn off load when desired current has been reached.

Experiment

9. **Run experiment**
    - Measure the electrolyte temperature before the experiment (should between 5-8 °C, ≤ 6°C). Take out the thermometer after directly!
    - Place then the taped sample prepared before into the electrolyte.
    - In the Acquisition software → Name experiment → Press run to start recording.

- After 5 seconds press the VAC button and thereafter the load button.
- Observe the voltage-time graph (i.e. V-T) until desired time point of 300 seconds/samples.
- Turn off load at time point + 5 seconds
- Press stop button on software
- Take out the samples and cut them, so that the samples no longer contain tape.
- Put the remaining sample inside a beaker glass.
- Clean the samples with running tap water for 1 minute
- Rinse the samples twice with demineralized water.
- Dry samples and store them properly.

10. Export data

- Export (desktop) → Run → Find foler (D: …) → Read
- Open txt file and create V-T graph in Excel
- Prepare for new experiment in acquisition screen: Clear chart. Reinitialize voltage and samples.

Turn off equipment

⇒ Interface, oscillator, power supply and cooling system.

Cleaning

- Cathode - Place cathode in running tap water for 5 minutes.
- Clean inside and outside with sponge
- Rinse with demineralized water
- store in 50% sulfuric acid.

NOTE: Don't overfill the acid tank, max. 2/3 of tank filled.

- Electrolyte –(can be stored for max. 2 weeks in fridge). Waste: alkaline inorganic
- Aceton/ethanol/acid - In designated tanks and replace when necessary
- PEO beaker - Clean with demineralized water
- Glasses Clean in sink with detergent

Sterilization (only for antibacterial experiments)

- Place samples on watch glass
- Sterilize samples in oven for 1 hour at 110°C
- Insert samples in the sterile tagged bags.

Materials & Equipment (15)

1. PEO Set-up:
   - Power supply
   - Oscillator
   - Interface
   - Cooling system
2. Electrolytic double-wall glass for PEO beaker
3. Calcium acetate
4. Calcium glycerophosphate
5. Antibacterial NPs
6. Ti6Al4V SLM mini-implant
7. Previously oxidized titanium substrate

8. Sample holder with crocodile clippers
9. Waterproof tape
10. Spray bottles containing:
    - Demineralized water
    - Ethanol
    - Acetone
11. Beaker glass
12. Watch glass
13. Tweezers
14. Scissors
15. Stopwatch

Protocol 2: Protocol Scanning Electron Microscopy

Aim. Taking microscopic images of surfaces.

Startup

- Key to start position (will go to 1 afterwards automatically)
- Wait until blinking gone
- Start PC

Sputtering samples

- Prepare samples
    - (If in resin, this resin should be electroconductive)
- Put samples on double sided carbon tape
- Gold sputter
    - Samples in sputter device
    - Switch on device
    - Press lightly on lid
    - Wait till the arrow at 40
    - Press leak
    - Wait till arrow at 40
    - Press start
        - Sputtering initiated (18sec)
    - Wait till switches off
    - Switch off sputter device
    - Wait till sound gone
    - Open lid (be careful not to touch inner ring of lid!)

Insert samples in SEM

- On SEM press Vent (to de-vacuum)
- Wat till Vent green
- Pull out holder microscope
- Measure, if your sample protrudes above holder (measure how much)
- Add protrusion (if applicable)
    - Adjust z-axis as indicated (standard at 10mm)

- Close holder in SEM
- Press Evac and wait until the blue blinking is gone
- Press Observe (ready to image)

Black control panel

- Press x/y to blue (so beam is fixed)
- Lowest magnification for orientation
- Drag with mouse or joystick to move around
- In this order
    - AF: autofocus
    - AS: autosigma
    - ACB: auto contrast/brightness
    - Note: when in Backscattering mode reverse order: ACB→AS→AF)
- If necessary: adjust focus/brightness manually
- Press button of magnification/focus > change to coarse (blue letters appear)
- Repress for fine

Software

- SRT: rotation sample (image rotation)
- Settings
    - Autosave: define folder
    - Also possibility to set the labels in your image (voltage, p.c. WD etc.)
- Double mouse click: comes in middle
- Higher voltage → higher detail (yet more charging/brightness)
- Mode
    - Fast/slow (less/more detail)
    - Press photo for photo
    - Automatic freeze

Saving images

- Press on settings

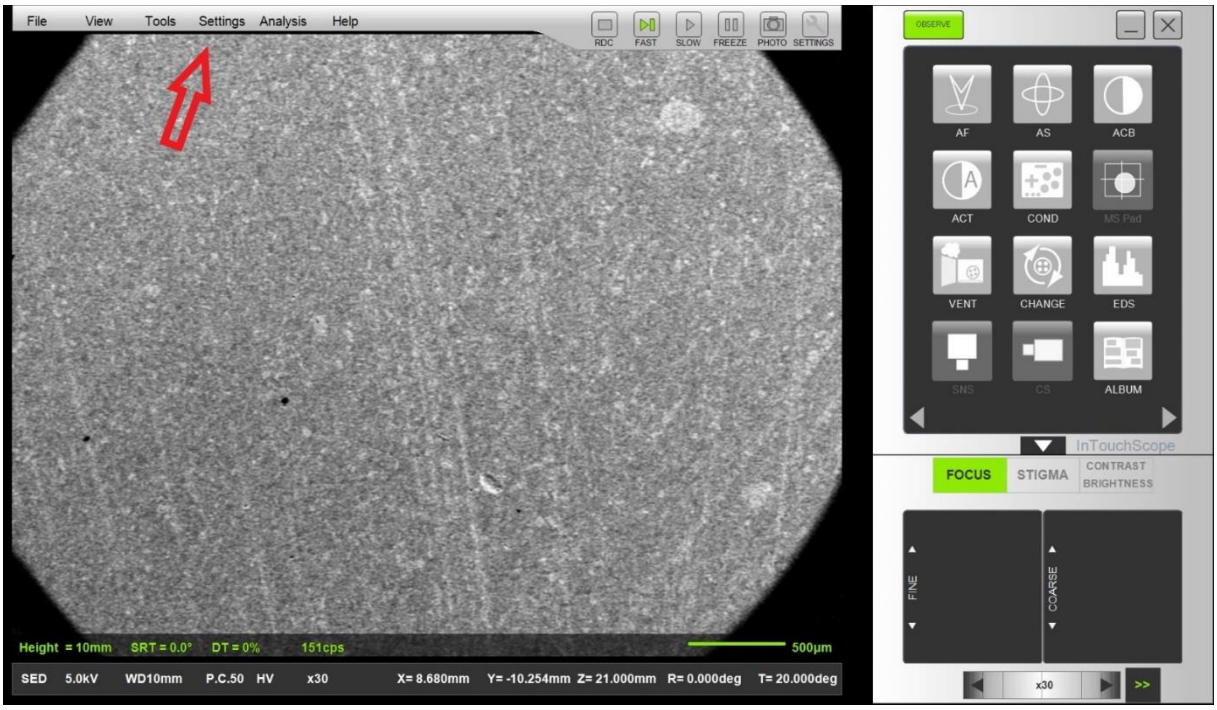

- Save the image in the right folder by pressing the dotted line in the section destination and choose the right map to save the images.

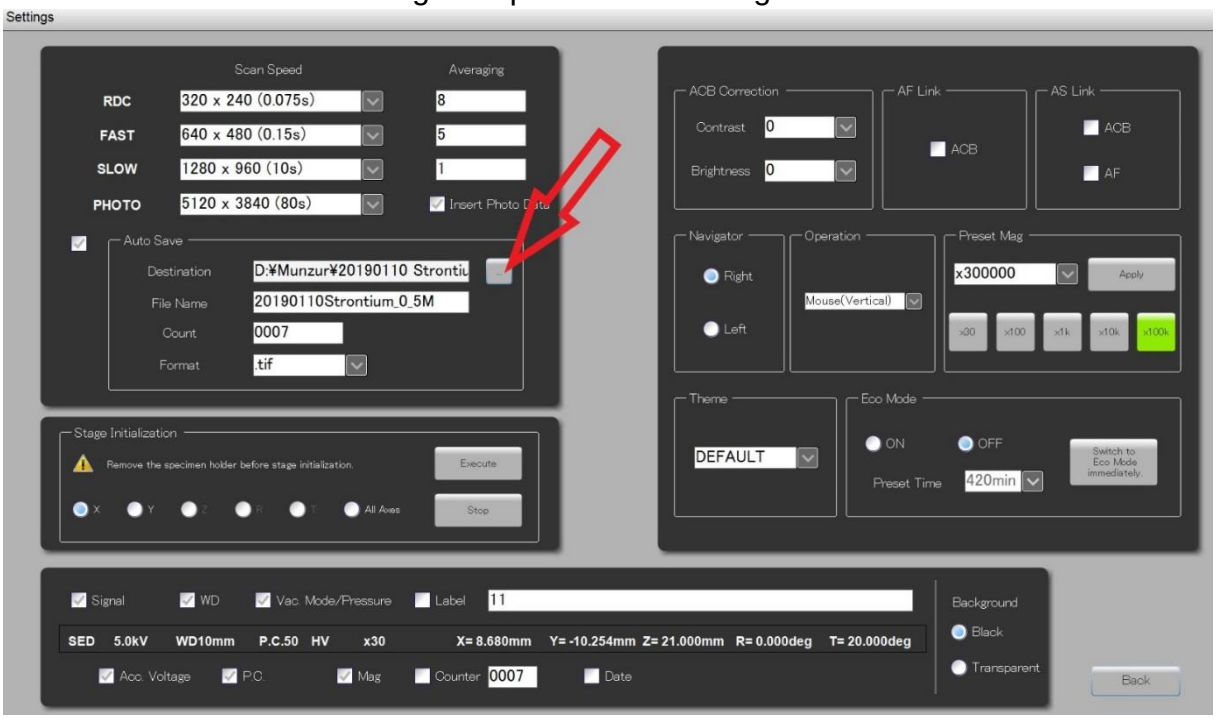

- Give it also a file name in the section file name
- Set count to 0001 (so the images are counted from 1)

Modes

- SED: secondary electron mode
- BEC: back scattering mode
- Switch between modes

- Click on mode
- Click on desired mode
- Check whether either BEC or SED appears in image

EDS

- WD (working distance) should be 10mm
- Use the EDS always in SEC mode and preferably between the 5kV and 10kV. So the filament don't burn-out too fast.
  - Defined by z-axis
- Map: scan in certain area
- Line: do in line
- Data
  - Select point or area
  - Click for spot
  - Start
  - Acquiring
  - Afterwards
    - Print > create > other program > save as
- Click observe to continue to normal SEM

Shut off sample

- Press Vent
- Take sample out
- Z-axis back to 10 (by default)
- Close
- Press Evac
- Turn key to 0

Protocol 3: Zone of inhibition

2018
Author: Melissa Tierolf

Aim. To test the inhibitory leaching activity of the antibacterial agents on the titanium substrate.

Procedure

<u>Day 1:</u> Experiment

1. Prepare fresh bacterial inoculum

- Use an inoculation loop to get a bacteria strain from blood-agar plate
  - ⇒ Tip a <u>single</u> bacteria colony once with an inoculation loop
- Suspend 1 colony in 3 ml fresh TSB medium in a 15 ml tube
  - ⇒ Inoculation loop in the TSB medium and press against the side of the tube so that all the bacteria are in the medium
  - ⇒ Vortex the tube
- Prepare also 3 ml TSB as control group without bacteria in a 15 ml tube
  - ⇒ Strain: MRSA USA300
- Incubate both tubes for ~3 hour at 37 °C '*shaking*'

- After ~3 hour vortex the tubes
- Measure the OD_{600nm}, and incubate till OD_{600nm}: 0.5
    - ⇒ In order to be sure that the bacteria are in 'log' phase
- Dilute the fresh cultures in TSB broth to OD_{600nm}: 0.01 (~1*10^7 CFU/ml)
- Measure the OD_{600nm} of the dilution to check the OD_{600nm}

NOTE: before measuring always vortex the tubes

2. Prepare LB-agar plates (in flow cabinet)

- Grab an LB-agar bottle (in solid-state)
- Put the bottle into the microwave
- Press *auto* button twice on the microwave, to select the program: *Def 2*
- Turn the dial to the amount of kilo that is going to be prepared, corresponding to number of LB-agar plates that should be prepared
    - ⇒ 1 LB-agar bottle = **1.3** kilo ≈ 20 LB-agar plates
    - ⇒ 2 LB-agar bottles = **2.6** kilo ≈ 40 LB-agar plates
- Turn on the program and wait until it is finished

NOTE: the content of the LB-agar bottle should be fully melted 'liquid' afterwards, otherwise restart the program.

- Turn on the flow cabinet
- Press the button 'ventilation' to turn it on
- Press the button 'A' to turn the alarm off
- Raise the glass and put it in its safe position
- Wait until the working cabinet is in its working mode – safe
- Press the light button to turn the light on
- Clean the working area with Ethanol
- Grab a few petri dishes and add the liquid LB-agar to the surface of those dished, approximately 2 ml in each petri dish

NOTE: the LB-agar in the petri dished should be homogenous distributed without bubbles.

- Allow the petri dishes with LB-agar to dry/cure

3. Spectrophotometer: measure the OD_{600nm} of bacteria suspension/dilution

- Set OD_{600nm}
- Calibrate by putting the control group 'without any bacteria strain' into the device and press the 0 ABS 100% T button
- After calibration, check if the settings are 600 nm and 0 A for the control group.
- If calibration is correct, the OD_{600nm} could be obtained for the fresh bacterial inoculum.

4. Prepare LB-agar plates with implants to determine zone of inhibition

- When the LB-agar plates has cured. Grab the agar-plates and label the agar-plates on the backside to the corresponding implant type
- Use a sterile swab 'cotton swab' to evenly distribute the bacteria suspension on the agar-plates.
    - ⇒ Use a new cotton swab for each plate
- Distribute the bacteria suspension according to the lay out presented in Appendix A
    - ⇒ Turn the plate each time with a quarter turn until the plate is completely covered with bacteria
    - ⇒ Swab from the inside to the outside of the plate AND not afterwards from inside to outside (<u>only one layer of bacteria</u>) – *one streak*

- Use tweezers and sterilize them by use of the burner
  ⇒ Open the gas tap first
- Place three similar implants next to each other using the lay-out presented in Appendix B
- Place plates in the incubator at 37°C overnight, no shaking overnight.

5. Prepare dilution series of the bacteria suspension OD_{600nm}: 0.01

- Use 96-wells plate
- Pipet 180 μl PBS in the first wells of all rows of the plate, except the top/first and last row
- In row A, pipet 100 μl **bacteria suspension** in the first well
- Take up 20 μl from the first well in row A and dispense in row B.
- Change the pipet tips
- With clean tips, mix the first well in row B by pipetting up and down (3 times suck up and spit out), then pipet 20 μl from the first well in row B (can be done with the same tips) to the first well in row C
- Repeat those steps for following rows until the last row (row G).

6. Inoculum check

- Grab blood-agar plate and label the plate on the backside including name, date and bacteria inoculum
- Pipet with a multi-channel (7 channels) 10 μl suspension of the dilution series from the 96 wells plate on the blood-agar plate
  ⇒ Mix the suspension
  ⇒ Keep the plate in 45 degrees and press the tips loosely on the plate.
  ⇒ Let the suspension run over the plate as 'lines'
  ⇒ Pay attention: lines may not flow into each other

NOTE: the blood-agar plate label should always be on top 'up', to ensure that row A/OD_{600nm}: 0.01 is the left column on the blood-agar plate and the right column corresponds to row G/OD_{600nm}: 0.00000001 (See Appendix C)**.**

- Place plate in the incubator at 37°C overnight, no shaking overnight.

NOTE: steps needs to be done to check the amount of CFU (i.e. bacteria) present in the dilution, which should be ~1*10^7 CFU/ml

<u>Day 2:</u> Acquisition of data: zone of inhibition (ZOI) and bacteria inoculum

7. Digitizing the data: Image Quant LAS 4000

- Start up the computer present in the lab and to get access fill in the password.
- Start up the device 'Image Quant LAS 4000'
- Open the program **Image Quant LAS 4000**
  ⇒ Set Exposure Type → Precision
  ⇒ Set Exposure Time → Manual → Set to 1/15 seconds.
  ⇒ Set Sensitivity/resolution → Standard
  ⇒ Open Method/Tray position → Method → Digitization → Epi-illumination
  ⇒ Set Tray position → 1
  ⇒ Open Focusing → Brightness → Set to 7 or 9
  ⇒ Press start
  ⇒ Save the data and repeat the procedure.

- **Change the following settings for acquisition of the bacteria inoculum data**
  ⇒ Set Exposure Time → Manual → Set to 1/8 seconds.
  ⇒ Open Focusing → Brightness → Set to 7

NOTE: the blood-agar plate label should always be on top 'up', to ensure that row A/OD_{600nm}: 0.01 is the left column on the blood-agar plate and the right column corresponds to row G/OD_{600nm}: 0.00000001 (See Appendix C)**.**

8. Data acquisition: Image J

- Open the program **Image J**
  ⇒ Drag the picture of interest to the Image J main frame and drop
  ⇒ Open Analyze → Set Scale to → and press on OK
    - Set Distance in pixels: 136.45
    - Known distance: 1.0
    - Pixel aspect ratio: 1.0
    - Unit of length: cm
  ⇒ Select 'Polygon selections' to select the area of the zone of inhibition
  ⇒ Press command/ctrl M to get the results of the area for n=3
  ⇒ Click 'Results' and 'Summarize' to obtain values for the Mean and SD
  ⇒ Store the results in the excel format

Materials & Equipment (15)

1. Bacteria strain: MRSA USA300
2. LB-agar plates (10 ml agar-plate)
3. 96-wells plate
4. Ti6Al4V SLM mini-implant with antibacterial agents (NPs)
5. Bottle containing:
   - TSB broth
   - LB-agar
6. Spray bottles containing ethanol
7. Inoculation loop
8. Cotton swabs
9. Tweezers
10. Incubator
11. Flow cabinet
12. Spectrophotometer
13. Calculator
14. Computer
15. Image Quant LAS 4000

Appendices

Appendix A

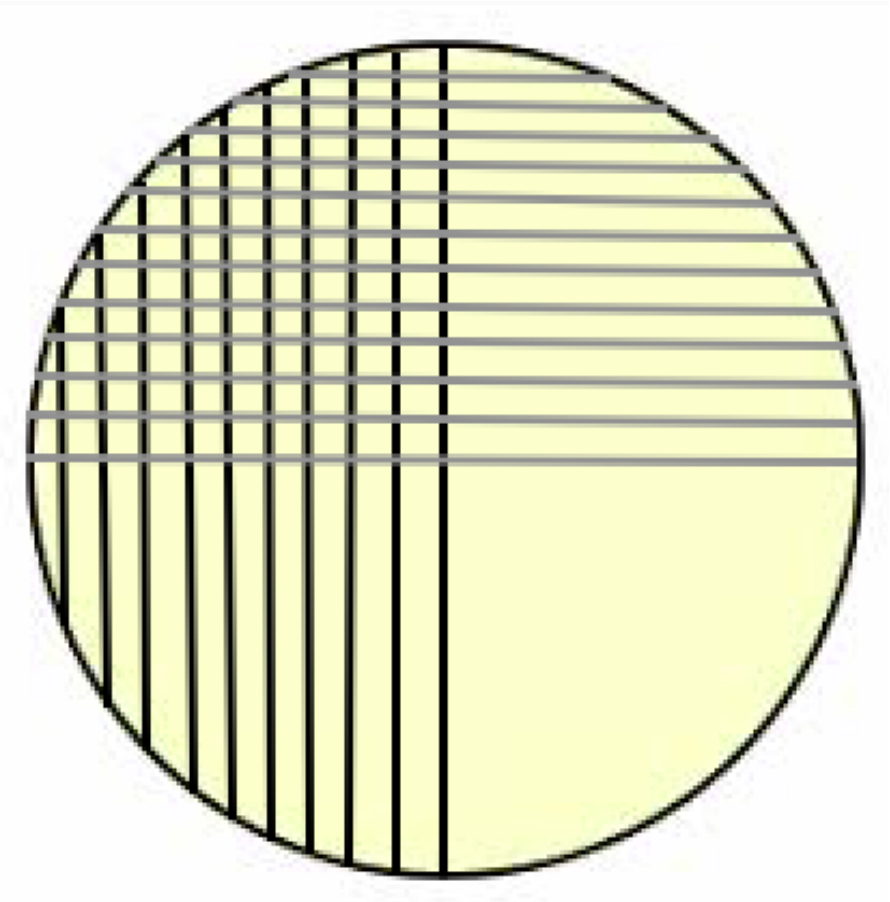

Figure A. Bacteria distribution suspension method: Turn the plate each time with a quarter turn until the plate is completely covered with bacteria Swab from the inside to the outside of the plate AND not afterwards from inside to outside (only one layer of bacteria) – *one streak*

Appendix B

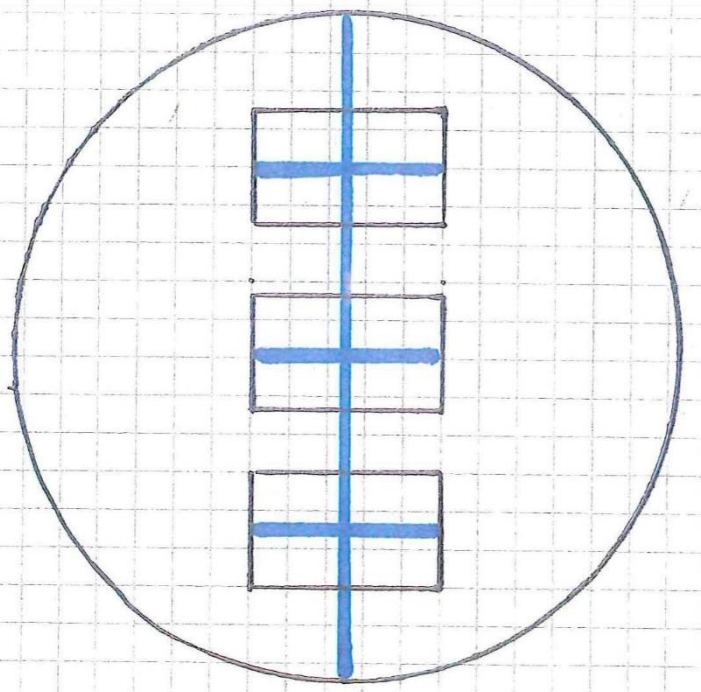

Protocol 4: Direct contact assay

Raisa Grotenhuis,
February 2019
TU Delft

Aim. Testing contact killing of solid and porous titanium surfaces

Day 1

1. Tip one colony of USA300 from a fresh plate and dilute it in 3 mL TSB and make a control tube without bacteria.
2. Vortex and incubate for ± 2 h at 37°C while shaking
3. Measure the OD at 600 nm. It should be above 0.2.
4. Prepare inoculum of 6.7 * 10^5 CFU/ml (OD 0.01 = 10^7/ml) for discs and 1.6 * 10^6 CFU/ml for the porous implants.
    a. **STEP 1** Prepare inoculum of 10^7 CFU (if OD = 0.1 → 0.1/0.01= 10 so ten times dilution. If you want a bacterial solution of 3 mL , 0.3 mL is bacteria and 2.7 mL is TSB)
    b. **STEP 2 for discs:** Dilute from 10^7 to 6.7* 10^5 → dilute 15 times.
    STEP 2 for implants: **:** Dilute from 10^7 to 1.6* 10^6 → dilute 6 times.
5. Prepare clamps with 4 mini-implants placed next to each other.

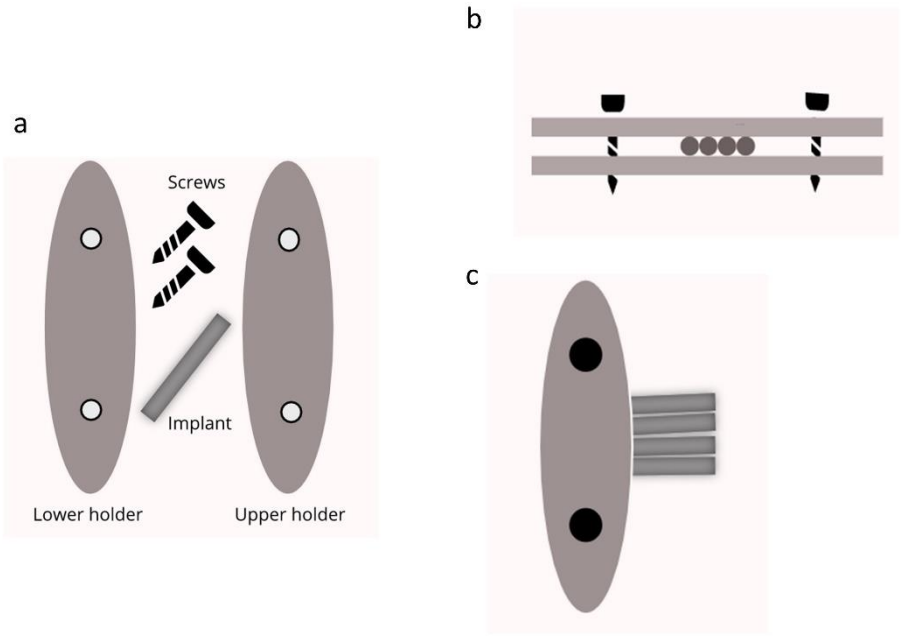

6. Pipet onto disks and mini-implants (n=3 per group)
    a. Pipet 40 µL (4 * 10^4 CFU) of the bacterial culture onto the middle of the disk
    b. Pipet 15 µL (2.5 * 10^4 CFU) onto mini-implants.
7. Cut parafilm
    a. place a circular piece (slightly smaller than the diameter of the disc, around 20 mm) on top of the inoculum and disc
    b. Place a piece of 2 mm by 10 mm onto mini-implants
8. Place 3 disks or mini-implants of each condition into a petri dish
9. Put flask caps filled with humidified tissue into the petri dish to create humid environment
10. Plate serial dilution (1-10^{-6}) on blood agar plate to check inoculum. Add 10 µl to 90 µl PBS 6 times.

Day 2

1. Place each disk (with the parafilm) in 5 mL PBS (in 50ml tubes) and label them.
2. Place each mini-implant (4 per group) in 200 µL PBS (in 0.5 ml Eppendorf) and label them.
3. Sonicate for 3 minutes and vortex for 15 seconds
4. Prepare serial dilutions ($1 – 10^{-6}$) in duplicates in 96 well plates.
    a. Add 90 µl of PBS to rows B-G
    b. Add 100 µl of sonicated dilution into row A
    c. Pipette 10 µl from row A into row B with multichannel: pipette few times up and down in row A before transferring into row B
    d. Repeat step c for the other rows
5. Use a multichannel to pipet 10 µl of the dilutions onto blood agar plates and label them (each group is tested 3 times and is diluted 2 times in a 96-wells plate, so each group will have 6 blood agar plates)
6. Incubate overnight

Day 3

1. Take pictures with imageLAS and count CFU
2. Count back the number of CFU present on the disc or implant

Materials & Equipment

1. Bacteria strain: MRSA USA300
2. Blood agar plates
3. 96-wells plates
4. Ti6Al4V SLM mini-implants/discs with antibacterial agents (NPs)
5. Bottle containing:
    - TSB broth
    - PBS
6. Spray bottles containing ethanol
7. Inoculation loop
8. Pipets and pipet tips
9. Parafilm
10. Petri dishes
11. clamps
12. 45 ml tubes
13. Eppendorf tubes
14. Sonication bath
15. Tweezers
16. Incubator
17. Flow cabinet
18. Calculator
19. Image Quant LAS 4000

Protocol 5: Electron Paramagnetic Resonance

Aim. To measure the reactive oxygen species release from the SLM implants.

Procedure.

1. **Turning on the EPR device, Figure. C**
   - Turn on the water tap for cooling.
     - Turn tap one quarter clockwise
     - If multiple EPR machines on, water cooling may have to be adjusted
   - Turn on the console and wait for a few minutes.
     - Check on back of console if power is on
   - Turn on the power supply.
     - In console > open lower drawer
   - Turn on the PC.
     - User: epruser. Password: user@xepr
   - Open the Bruker Xenon software.
     - Connect to spectrometer

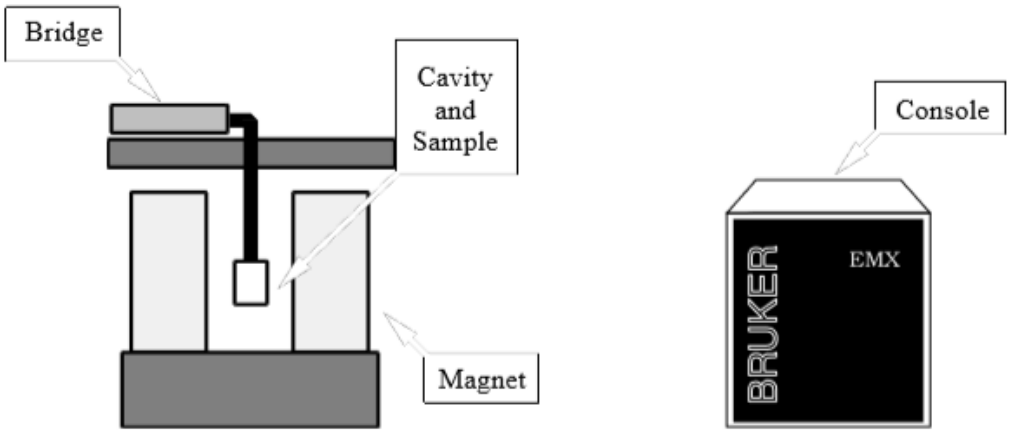

Figure. C General lay out of EPR instrument.

2. **Preparing samples**
   - Cut SLM implants into 0.5 cm and placed it into the capillary tube.
     - Capillary tubes are re-used
     - Note: in case of new sample (e.g. new material or nanoparticle) first perform measurement without adding DMPO solution
   - Prepare 100 mM DMPO solution in PBS.

- 22.632 mg in 10 ml
- Prepare 0.5ml aliquots and store in freezer

- Pipet 10 µL of the DMPO solution into the tube with implant in it.
  - With a syringe. First clean syringe 3x in demiwater
- Place the capillary tube in the cavity between the magnets (±7.2 cm), **Figure. C**.

3. Tune the microwave X-band frequency

- You can select to use parameters used in previous experiments
- Set on 'Tune' mode.
- Attenuation 10 dB.
- Adjust the frequency until the spectrum is in the middle.

  There is a guideline for it.
- Click on Auto tuning and wait until the color turns into green (tuned).

4. Start measurement.

- Insert sample with low power
  - Attenuation 60dB > low power

a. In case of new sample (e.g. new material, nanoparticle)

  - First do measurement <u>without</u> implant in PBS (background measurement)

- Settings:
  - 9.78 GHz frequency
  - 2500 G center magnetic field
  - 4799 G sweep width
  - 163.8 ms time constant
  - 160 ms conversion time
  - 5 G modulation amplitude
  - 100 kHz modulation frequency
  - 60 dB receiver gain
  - 30 dB attenuation
  - .. mW power

b. Measuring ROS

- Start with 1D Field Sweep to obtain the t = 0 seconds ROS release.
- Settings for the ROS measurements were described as following:
  - 9.78 GHz frequency

- 3486 G center magnetic field
- 100 G sweep width
- 163.8 ms time constant
- 160 ms conversion time
- 1 G modulation amplitude
- 100 kHz modulation frequency
- 60 dB receiver gain
- 10 dB attenuation
- 20 mW power

- Save the file.
- After that, using similar settings, start 2D Field Delay measurements.
- Set the measurements every 10 minutes and for 15 times.
    - *This is depending on how long the measurements need to be done.*
- Save the file.

5. Stop measurement.

- Set attenuation to 60 dB > resulting in low power
- Set to stand-by
- Wait few minutes before turning off water (magnets may still be warm)

Required Materials.

- Capillary tubes.
- Capillary pipets.
- SLM implants.
- PBS solution.
- DMPO.

Protocol 6: EPR with bacteria

Raisa Grotenhuis
May 2019

Aim. Measuring reactive oxygen species generation of implants in contact with bacteria.

Day 1

1. Tip a colony of *S. aureus* and dissolve in 10 mL BHI broth
2. Incubate overnight (18 h) at 37˚C while shaking.

Day 2, bacteria in PBS

1. Dilute inoculum 10 times in order to measure OD.
2. Measure the OD (and calculate back , times 10) and dilute up to OD 1.0 ($6.7 * 10^8$ CFU/mL) in 2 mL Eppendorf tube with BHI.
3. Centrifuge at 12000 rpm for 1 minute. Check whether bacteria are visible.
4. Pipette BHI out and replace by same amount of PBS. Vortex tube so the bacteria are spread in PBS.
5. Go to EPR room.
6. Add 3 µL of inoculum in PBS to capillary ($2*10^6$ CFU)
7. Add 10 µL DMPO
8. Add implant
9. Start measurements directly (so you know directly what happens after contact between implant and bacteria).
10. Make 2D plots (time/delay should be set before start). See EPR protocol for further instructions.

Day 2, adherent bacteria

1. Prepare BHI agar plates by melting a bottle of BHI agar (in microwave) and spread it over 20 petri dishes.
2. Dilute inoculum 10 times in order to measure OD.
3. Measure the OD (and calculate back , times 10) and dilute up to OD 0.1 ($6.7 * 10^7$ CFU/mL) in 2 mL Eppendorf tube with BHI.
4. Place 4 implants from each group in 100 µL of the inoculum ($6.7 * 10^6$ CFU) in 0.5 ml tubes.
5. Incubate for 2 h at 37˚C.
6. Takes implants out and wash in PBS
7. Place 3 implants of each group in Eppendorf tube in 200 µL PBS and sonicate for 1 minute and vortex for 15 seconds.
8. Prepare serial dilutions ($1 – 10^{-6}$) in duplicates in 96 well plates.
    a. Add 90 µl of PBS to rows B-G
    b. Add 100 µl of sonicated dilution into row A
    c. Pipette 10 µl from row A into row B with multichannel: pipette few times up and down in row A before transferring into row B
    d. Repeat step c for the other rows
9. Use a multichannel to pipet 10 µl of the dilutions onto BHI agar plates and label them (each group is tested 3 times and is diluted 2 times in a 96-wells plate, so each group will have 6 BHI agar plates)
10. Incubate overnight.
11. Take the 4^{th} implant for EPR measurements. Go to the EPR room and add the implant (with adherent bacteria) and 10 µL DMPO to capillary and start 2D measurements (time/delay should be set before start). See EPR protocol for further instructions.

Day 3, adherent bacteria

1. Take pictures of BHI plates and count CFU.

Required materials

- Colony of *S. aureus* RN4050
- SLM implants
- BHI
- PBS
- 96 wells plate
- Pipettes
- BHI agar
- Petri dishes
- Eppendorf tubes
- Sonicator
- Vortex
- Centrifuge